

CHE4045Z – Chemical Engineering Project



FINAL REPORT

INVESTIGATING SYSTEM KINETICS IN BIO-CHEMO TANDEM SYSTEMS

CENTRE FOR BIOPROCESS ENGINEERING RESEARCH

Group BI

Nikhil Mistry and Joe Payne

Supervisors

Dr Thanos Kotsiopoulos, Deborah Chikukwa and Prof Sue Harrison

SYNOPSIS

This project aims to determine the feasibility of combining the bioactivation of alkanes with the chemical oxidation of alcohols in a one-pot tandem system. Alkanes are a widely available feedstock and are difficult to activate using traditional catalysts due to the poor selectivity achieved and harsh conditions required. The use of biological enzymes for this activation however results in a highly selective reaction to primary alcohols. The lower value alcohol needs to be valorised through oxidation in a separate reaction to generate a more profitable product. This oxidation of the primary alcohol to a commercially lucrative aldehyde is completed using metallic nanoparticles. Coupling the two processes offers the versatility of chemocatalytic systems with high selectivity and mild conditions of biocatalytic processes. A one-pot system is the ideal configuration in which to combine these two distinct reactions as it will reduce capital requirements and potentially make the process more efficient.

However, having both reactions in the same one-pot system implies that they will take place under the same conditions and thus a feasible operating window needed to be determined. It is for this reason that the kinetics for each step of the tandem process were investigated. Three mechanisms were proposed to describe the bioactivation of alkanes to alcohols, where the physical parameters for each were regressed by comparing the alcohol concentration predicted by the models to data obtained experimentally. It was found that the model describing reaction limitation due to the mass transfer of substrate from the organic phase to the aqueous phase was the most accurate and thus is likely what occurs in reality.

For the chemical oxidation of the alcohol in the second step of the process, two different mechanisms were proposed. The first generates the desired aldehyde product but also leads to the reformation of the initial alkane through an undesired side reaction. The second mechanism also produces an aldehyde but results in the aldehyde potentially undergoing further oxidation to a carboxylic acid. As with the alkane activation models, these mechanisms were compared to experimental data and their reaction constants were determined accordingly. It was discovered that the second mechanism better describes the data obtained and thus this is what was used in the modelling of the one-pot and two-pot systems.

These developed models were used to simulate two-pot and one-pot processes to obtain an idea into how viable the one-pot approach would be. The two-pot process was designed to guarantee that the alkane activation operated at 20°C to be suitable for the microorganism, with the second step also taking place at that temperature to ensure high selectivity to the aldehyde and that the rates of alcohol production and consumption could be matched to obtain a continuous process. Ultimately, the result of the reactor modelling was that two-pot process had a total residence time of 210 h, producing a 0.028 M aldehyde product with a selectivity of 5.2. The design choices for the one-pot process were made to ensure that a highly selective aldehyde was produced with the maximum possible yield. This was achieved by having one reactor vessel, again operating at 20°C to favour both reactions, with a residence time of 83 h. The final output of the one-pot system is an aldehyde concentration of 0.036 M at a selectivity to carboxylic acid of 6.0. The improved performance in the one-pot results in a potential reduction in capital expenditure of 52%, an increased product revenue of 29% and reduced downstream processing costs due to improved selectivity. This indicates a potential feasibility of the one-pot route for alkane activation and valorisation, but this needs to be validated through a more comprehensive techno-economic analysis.

PLAGIARISM DECLARATION



| | | | |
|--|--|----------------|------------|
| CHE4054Z | | | |
| Chemical Engineering Project | | | |
| 2020 | | | |
| Student Number | MSTNIK002 | | |
| | PYNERI001 | | |
| Date Completed | 10/12/2020 | Date Handed-In | 10/12/2020 |
| DECLARATION 1. We know that plagiarism is wrong. Plagiarism is to use another's work and to pretend that it is one's own 2. This report is our own work 3. We have not and will not allow anyone to copy this work with the intention of passing it off as his or her own work | | | |
| Signature |  | 10/12/2020 | |
| |  | 10/12/2020 | |

TABLE OF CONTENTS

| | |
|---|----|
| 1. INTRODUCTION | 1 |
| 2. LITERATURE REVIEW..... | 2 |
| 2.1. Alkane activation | 2 |
| 2.2. Alcohol oxidation | 7 |
| 2.3. Orthogonal tandem catalyst | 10 |
| 2.4. Objectives..... | 12 |
| 2.5. Hypotheses | 12 |
| 2.6. Key questions | 12 |
| 3. RESEARCH APPROACH AND MODEL DEVELOPMENT..... | 13 |
| 3.1. Methodology | 13 |
| 3.2. Alkane activation kinetic model development..... | 14 |
| 3.2.1. Data sourcing | 14 |
| 3.2.2. Potential reaction mechanisms..... | 14 |
| 3.3. Alcohol oxidation kinetic model development..... | 16 |
| 3.3.1. Data sourcing | 16 |
| 3.3.2. Potential reaction mechanisms..... | 17 |
| 3.3.3. Formulation of kinetic models | 18 |
| 3.4. Reactor modelling..... | 21 |
| 4. RESULTS AND DISCUSSION | 23 |
| 4.1. Alkane activation kinetic modelling and parameter estimation | 23 |
| 4.2. Alcohol oxidation kinetic modelling and parameter estimation | 25 |
| 4.3. Two-pot system | 27 |
| 4.4. One-pot system | 30 |
| 4.5. Model limitations..... | 33 |
| 4.6. Comparison of modelling results..... | 33 |
| 5. CONCLUSIONS..... | 35 |
| 6. REFERENCES | 37 |
| APPENDIX A: Detailed experimental methods..... | A |
| APPENDIX B: Alcohol oxidaton parameter esitnation results | F |
| APPENDIX C: Captial costing sample calculations | G |

| | |
|---|---|
| APPENDIX D: Data management declaration | H |
| APPENDIX E: Ethics clearance | I |

LIST OF FIGURES

| | |
|---|----|
| Figure 1: Distribution of products as a result of chemical activation of octane from (CChange, 2020). | 2 |
| Figure 2: Mechanism of alkane hydroxylation using CYP153 (Soussan et al., 2016)..... | 3 |
| Figure 3: Illustration of a) interfacial adsorption model and b) mass transfer limitation. | 5 |
| Figure 4: Reaction mechanism for the oxidation of alcohols presented by a) (Davis et al., 2013) and b) (Galvanin et al., 2018)..... | 7 |
| Figure 5: Classification of one-pot processes including multiple catalytic transformations (Fogg & Santos, 2004). | 10 |
| Figure 6: Research method used in the study | 13 |
| Figure 7: Comparison of proposed models for high initial substrate concentrations. Data obtained from (Centre for Bioprocess Engineering Research, 2020)..... | 24 |
| Figure 8: Comparison of proposed models for low initial substrate concentrations. Data obtained from (Centre for Bioprocess Engineering Research, 2020)..... | 25 |
| Figure 9: Comparison of proposed models for alcohol oxidation over a Pd ₈₀ /Au ₂₀ catalyst to experimental data obtained from (Villa et al., 2009). | 26 |
| Figure 10: Simple representation of two-pot process..... | 27 |
| Figure 11: a) Exit alcohol concentration as a function of residence time. b) Concentration profiles for 1-octanol and octane in the alkane activation reactor. | 28 |
| Figure 12: a) Matching rate of alcohol formation to alcohol consumption at different temperatures as a function of residence time. b) Selectivity to the aldehyde as a function of temperature. | 29 |
| Figure 13: a) Selectivity to the aldehyde as a function of the aeration rate. b) Concentration profiles for octanal and octanoic acid in the alcohol oxidation reactor. | 30 |
| Figure 14: Simple representation of one-pot process. | 31 |
| Figure 15: a) Selectivity to the aldehyde at different residence times as a function of aeration rate in a one-pot system. b) Exit aldehyde concentration as a function of residence time in the one-pot system. | 31 |
| Figure 16: Concentration profiles in the one-pot system for a) octanal and octanoic acid and b) octane and 1-octanol. | 32 |
| Figure A1: Conversion of 1-octanol raw data (Villa et al., 2009) | E |

LIST OF TABLES

| | |
|--|----|
| Table 1: Full reaction mechanism for Model 0 along with equilibrium equation for each reaction with the rate limiting steps shown in bold (Galvanin et al., 2018)..... | 18 |
| Table 2: Full reaction mechanism for Model 1 along with equilibrium equation for each reaction with the rate limiting steps shown in bold (Davis et al., 2013)..... | 20 |
| Table 3: Summary of parameter estimation for Michaelis-Menten model. | 23 |
| Table 4: Summary of parameter estimation for mass transfer model..... | 23 |
| Table 5: Summary of parameter estimation for interfacial adsorption model. | 23 |

| | |
|--|----|
| Table 6: Statistical results of proposed alkane activation models. | 24 |
| Table 7: Summary of statistical analysis for the comparison of the proposed models for alcohol oxidation | 27 |
| Table 8: Summary of capital costs and potential revenues for each reactor system. | 34 |
| Table A1: Raw experimental data for octane hydroxylation. | A |
| Table A2: Continued raw experimental data for octane hydroxylation. | B |
| Table A3: Growth and expression procedures. | C |
| Table A4: Medium composition. | C |
| Table A5: Description of bacterial strain used for octane hydroxylation. | C |
| Table A6: Description of terms used in Table A5. | D |
| Table A7: Description of cell preparation procedure. | D |
| Table A8: Description of inoculum preparation procedure. | D |
| Table A9: Concentration-time data for the oxidation of 1-octanol | E |
| Table B1: Parameters for Model 0 as a result of non-linear regression | F |
| Table B2: Parameters for Model 1 as a result of non-linear regression | F |
| Table C1: Summary of information required to size each reactor | G |

NOMENCLATURE

| Item | Description |
|------------------------|---|
| AH | Alkane hydroxylase |
| Au | Gold |
| CSTR | Continuous stirred tank reactor |
| CYP | Cytochrome P450 |
| <i>D.Desulfuricans</i> | <i>Desulfovibrio desulfuricans</i> |
| <i>E. coli</i> | <i>Escherichia coli</i> |
| K | Langmuir adsorption constant |
| k_{cat} | Turnover number |
| k_i | Chemocatalyst rate constant |
| k_{La} | Mass transfer coefficient |
| K_m | Michaelis constant |
| m | Partition coefficient |
| NAD(P)H | Nicotinamide adenine dinucleotide phosphate |
| NP | Nanoparticle |
| ODE | Ordinary differential equation |
| Pd | Palladium |
| τ | Residence time |

GLOSSARY

| Item | Description |
|------------------|---|
| Active sites | Location on catalyst where a catalytic process occurs. |
| Aeration rate | Amount of oxygen added to a process. |
| Alkoxide | The conjugate base of an alcohol. |
| Bare module cost | Capital cost of unit operations. |
| Bio-fabrication | Production of complex biological structure from raw biomaterials. |
| Chi-square test | Test to measure the ability of a model to predict experimental data. |
| Cofactor | Non-protein chemical compound which is required to ensure an enzyme's activity. |
| Enzyme | Proteins which act as biological catalysts. |

| | |
|------------------------------|--|
| Enzyme inhibition | Decrease in enzyme activity and productivity. |
| Geminal diol | An organic molecule with two hydroxyl groups. |
| Hydrophobic | Physical property of a substance which is repelled by water. |
| Isothermal | A process in which the temperature of the system remains constant. |
| Langmuir-Hinshelwood | Approach to develop a microkinetic model for a reaction mechanism occurring over a chemical catalyst. |
| Levenberg-Marquardt | Minimising algorithm used to solve least squares problems. |
| Microorganism | Living organisms which are only visible under a microscope. |
| Monooxygenase | Enzymes that incorporate a hydroxyl group into a molecule by a metabolic pathway. |
| Nelder-Mead | Numerical method used to find the minimum of a function. |
| Operon | A unit comprised of linked genes used to regulate other genes for protein synthesis. |
| Pearson Correlation | Correlation coefficient to represent the relationship between two variables. |
| Periplasmic space | Concentration matrix in the space between the inner cytoplasmic membrane and bacterial outer membrane. |
| Recombinant DNA | DNA molecules formed by recombining genetic material from multiple sources. |
| Selectivity | The ratio of desired to undesired product in a reactor effluent. |
| Yield | The number of moles of product produced in relation to number of moles of reactant consumed. |
| β -Hydride elimination | The transfer of a hydride from the β position to the centre of a molecule. |

1. INTRODUCTION

The availability of easily accessible alkanes in the form of natural gas, petroleum products and as the result of Fisher-Tropsch processes make them an area of huge potential for the source of other higher-value organic compounds. However, their inert nature has made this valorisation impractical, economically and environmentally, due to the low yields and harsh conditions required, even with the addition of a chemical catalyst. This has created the opportunity for the use of biocatalysts such as CYP153A6, a cytochrome P450 (CYP) monooxygenase.

These monooxygenases are able to hydroxylate the alkane substrate with high selectivity to the primary alcohol, which is appealing due to the difficulty of terminal activation. Although the conversion of these reactions is still minimal, the product can be generated at much lower temperatures making it a more feasible process. However, the alcohol produced has a lower market value than the alkane substrate. This creates the requirement for further oxidation of the primary alcohol into an aldehyde product, which is more valuable due to its applications in fine chemical synthesis. There has been a great deal of progress in the oxidation of alcohols using a variety of different metal catalysts, including the use of bio-fabricated Au and Pd nanoparticles.

By coupling these two processes, the low value alkane source can be converted into a high value aldehyde product. However, the purpose of this research project is to attempt to combine the two reactions into a one-pot process using orthogonal tandem catalysis. Using a one-pot process reduces the initial capital requirements by eliminating the need for two separate reactors and associated utilities. However, this brings about a different set of challenges such as the potential of catalyst inactivation due to interactions between the different catalysts and attempting to find a suitable set of conditions for both reactions to proceed efficiently within the same environment.

The aim of the study is to obtain experimental data for both individual reactions and investigate potential models in literature which are able to describe them. Once these models have been developed, they will be compared to determine any suitable reaction conditions allowing both processes to take place with a high degree of efficiency. In this way, the opportunities presented by a one-pot system will be investigated and therefore a comparison can be made between the one-pot and two-pot approaches to evaluate the future potential of the one-pot orthogonal tandem system.

2. LITERATURE REVIEW

2.1. Alkane activation

Alkanes consist exclusively of strong C-C and C-H bonds within their molecules, making them very stable and almost completely inert. The large quantity of alkanes found in natural gas, mining and produced through Fisher-Tropsch synthesis have been historically undervalued as carbon feedstocks (Soussan et al., 2016). Different types of chemical catalysts have been tested to use these alkanes in the generation of a more valuable product. Homogenous catalysts use metal complexes to attempt to imitate the active site of an enzyme produced by a microorganism. However, this results in challenges in attempting to recover the expensive catalyst and poor regio-selectivity resulting in a wide distribution of products (Soussan et al., 2016). Heterogeneous catalysts make catalyst recovery more achievable, however low yields are still observed even though there have been attempts to improve the selectivity of the reactions (Soussan et al., 2016). An example of the wide product distribution achieved when various chemical catalysts are used to activate an octane feedstock can be seen in Figure 1 below. Having such large a range of components produced makes isolating valuable ones difficult and significantly increases the costs of any downstream processing units required.

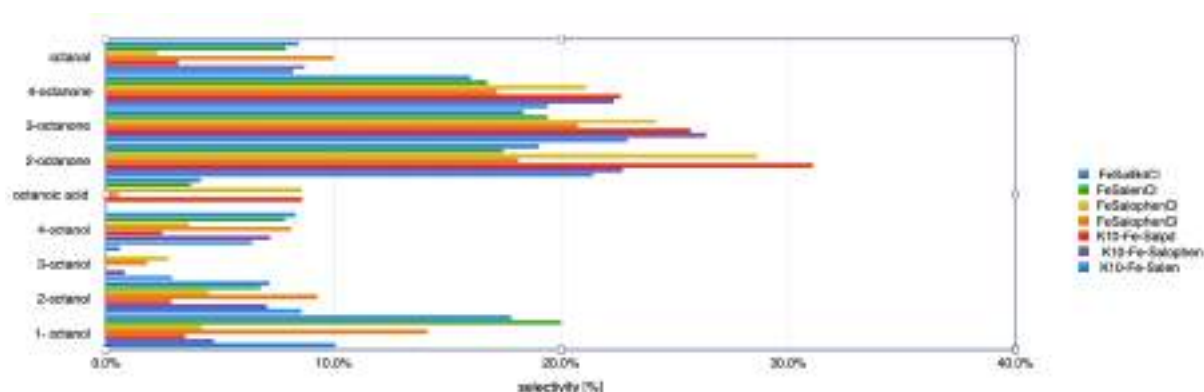


Figure 1: Distribution of products as a result of chemical activation of octane from (CChange, 2020).

The impracticality of using a chemical catalyst has resulted in the investigation into the potential of microorganisms to be used as biocatalysts. Many different microorganisms have been identified which are able to selectively utilise alkanes as an energy source in their metabolic processes under mild reaction conditions (Soussan et al., 2016). Specifically, certain organisms are able to hydroxylate alkane substrates into alcohols, utilising alkane hydroxylase (AH) enzymes to facilitate this conversion. One of the groups of AHs which have been studied are the cytochrome P450 monooxygenases (CYPs) (Soussan et al., 2016). CYPs have drawn a great deal of attention due to being able to hydroxylate a wide range of alkane substrates. When using CYPs, a NAD(P)H cofactor and oxygen are required for hydroxylation to take place. Expressing the enzyme in a recombinant host cell allows for the regeneration of this cofactor through the cell's metabolic process, a protected environment for the catalyst and the possible expression of the reductase and the mediator (Lundemo & Woodley, 2015).

Although CYPs can hydroxylate alkane substrates more selectively than other chemical catalysts have been shown to, it is still a struggle to achieve high yields of the product using these biocatalysts. Being able to achieve a reaction yield of more than 90% with a product concentration of at least 20 g.L⁻¹ is seen as being necessary to ensure a process' feasibility (Lundemo & Woodley, 2015). However, the majority of investigated CYPs are unable to achieve this target. This introduces the requirement for process optimisation which can be applied to improve the product concentration of a functioning biocatalyst system. The choice in host cell can be optimised, the catalyst could potentially be immobilised and the strain of CYP could be genetically modified to improve its performance (Lundemo & Woodley, 2015).

Utilising a whole cell culture to express the monooxygenase does result in potential mass transfer limitations through the cell membrane, limiting the rate of the hydroxylation reaction (White et al., 2017). This obstacle can be overcome through the permeabilisation of the membrane, genetic mutation of the host cell or the simultaneous expression of membrane transport proteins to assist in the transfer of the alkane substrate. The effects of mechanically breaking the cell were investigated by White et al. (2017) and it was found that permeating the cell wall resulted in a reduced rate of hydroxylation due to the release of cofactors into the aqueous phase. Therefore, the permeation of the cell needs to be coupled with the additional expression of a dehydrogenase enzyme to appreciate the benefits of eliminating the mass transfer limitations through the membrane (White et al., 2017).

Out of the large variety of CYPs, the family of CYP153s can hydroxylate the terminal carbon present in the aliphatic alkane with a selectivity of over 95%. This is an advantage CYP153s have over alternative members of the CYP group and other AHs like alkane monooxygenases (alkB) (Olaofe et al., 2013). This makes them highly productive in generating primary alcohols which can then be further oxidised to form aldehydes. Other enzymes can be used to activate the alkanes to aldehydes without the requirement for the intermediate alcohol. However, a wider distribution of products is generated requiring energy intensive downstream processing. One limitation of using CYP153s as the biocatalyst for alkane activation is they predominantly hydroxylate short to medium length alkanes (C₄ to C₁₁) (Olaofe et al., 2013).

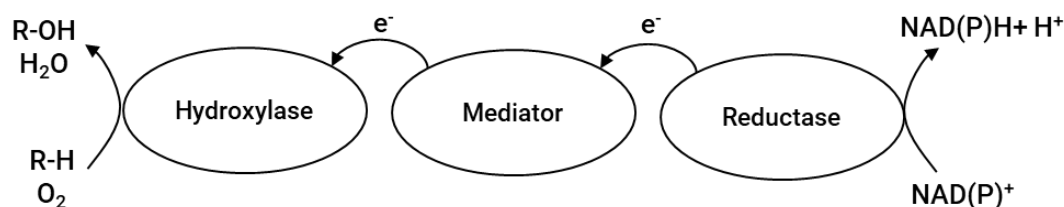


Figure 2: Mechanism of alkane hydroxylation using CYP153 (Soussan et al., 2016).

Another characteristic of CYP153s are that they are a member of class I CYPs, implying that in order to successfully hydroxylate the alkane substrate they require the use of a reductase and a mediator in the form of ferredoxin reductase and ferredoxin respectively (Soussan et al., 2016). The activation mechanism begins with the transfer of an electron from the cofactor

to the reductase, oxidising the cofactor to NAD(P)⁺. The electron then travels from the reductase to the CYP153 hydroxylase via the mediator. This electron breaks the covalent bond in the oxygen and reduces the one oxygen atom into water while the other is incorporated into the terminal carbon of the alkane, forming a primary alcohol (Soussan et al., 2016). This mechanism is represented in greater detail in Figure 2 above.

One of the members of the CYP153 family which has been investigated in detail is the CYP153A6 operon isolated from *Mycobacterium* sp. HXN-1500. Funhoff et al. (2006) expressed the CYP153A6 enzyme along with ferredoxin and ferredoxin reductase in a recombinant *Pseudomonas putida* host cell and successfully modelled the binding of the alkane substrate in the active site of the CYP153A6. Alkanes were shown to bind tightly with the hydroxylase enzyme, while cyclic and aromatic compounds had higher dissociation constants implying that they bind less well to the active site and that steric effects play a role in the effectiveness of the CYP153A6 enzyme (Funhoff et al., 2006). A further investigation into the mechanism of substrate binding was done using 3D modelling. This model demonstrated that the active site of the enzyme is hydrophobic in nature and that the terminal carbon of the alkane is positioned near the heme ion, allowing the hydroxylation reaction to take place at this location (Funhoff et al., 2006).

Another investigation was undertaken by Olaofe et al. (2013) into the effect of temperature on the performance of CYP153A6, with the enzyme, mediator and reductase expressed in an *Escherichia coli* (*E. coli*) host cell. The growth temperature was varied between 20°C and 37°C, with the incubation (period of enzyme expression) temperature set at 20°C. The growth temperature was found to have no significant effect on the concentration of CYP153A6 or the production of 1-octanol from octane. However, when the growth temperature was maintained for the incubation period, the concentration of CYP153A6 and 1-octanol decreased significantly for the higher temperatures (Olaofe et al., 2013). This implies that the system is less sensitive to the chosen growth temperature given that the incubation temperature is maintained at 20°C. When resting *E. coli* cells were used to determine their response to a varying temperature, it was determined that the greatest biocatalyst activity occurred at a temperature of 37°C. However, the higher temperature led to the instability of CYP153A6 thus preventing the accumulation of 1-octanol (Olaofe et al., 2013).

The effectiveness of CYP153A6 in the activation of the alkane substrates to primary alcohols can also be impacted by factors other than temperature. The addition of glucose to the system is necessary as part of the host cell's metabolic process and thus is linked to cofactor regeneration (Olaofe et al., 2013). However, if the concentration of glucose added is higher than 10 g.L⁻¹ it produces more of the acetic acid by-product which not only reduces the selectivity of the process but also partially inhibits the CYP153A6 (Olaofe et al., 2013). Another potential inhibitory compound is that of the alcohol product itself. Adding the 1-octanol prior to the hydroxylation reaction results in a significant decrease in the amount of octane converted, with no conversion observed with an initial 1-octanol concentration of 1.25 g.g_{DCW}⁻¹ (Olaofe et al., 2013). This inhibition can be mitigated in the proposed one-pot system as the alcohols produced will be immediately utilised to generate the final aldehyde product.

When considering the activation of alkanes using CYP153A6, by having a biphasic system, where the substrate is present in the organic phase and the monooxygenase is in the aqueous phase, the presence of non-enzymatic side-reactions can be limited by maintaining a low

concentration of substrate in the aqueous phase (Willeman et al., 2001). The nature of this biphasic system implies that the biocatalyst is active in the bulk aqueous phase or at the interface between the two phases (Straathof, 2003).

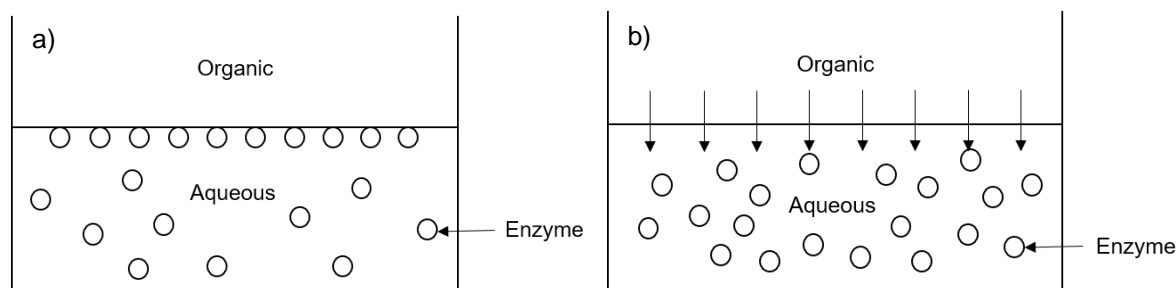


Figure 3: Illustration of **a)** interfacial adsorption model and **b)** mass transfer limitation.

In this two-phase system, the major influences on the rate of the hydroxylation reaction are the initial enzyme concentration in the aqueous phase, the substrate concentration in the organic phase and the size of the volume-specific interfacial area. The exact impact each of these variables has is explained by either the mass transfer model or the interfacial adsorption model (Straathof, 2003). An illustration of the two potential rate limiting models can be found in Figure 3 above (Straathof, 2003).

Mass transfer limitation occurs when the reaction rate of the organic substrate in the aqueous phase is faster than the transfer of the substrate from the organic to the aqueous. This limitation can be overcome by increased agitation in the reactor, decreasing the enzyme concentration or increasing the size of the interfacial area (Straathof, 2003). Depending on the nature of the enzyme and two phases, the biocatalyst adsorbing on the interface can potentially be inactivated or stabilised. Therefore, if required, the extent of enzyme adsorption can be decreased by reducing the size of the area or the initial enzyme concentration (Straathof, 2003).

Because the alkane substrate is nonpolar and thus does not readily transfer from the organic to the aqueous phase, the first step in building a model (for either the mass transfer or interfacial adsorption cases) is to relate the rate of the reaction to the change of substrate concentration in the organic phase, shown in Equation 1 (Straathof, 2003).

$$-\frac{dc_A^{org}}{dt} = \frac{V^{aq}}{V^{org}} r_A \quad (1)$$

The key is to relate the rate of the equation to the three previously mentioned variables which have the greatest influences on its magnitude. This relation is different for the two proposed models. However, these models are both based upon the Michaelis-Menten equation which is seen in Equation 2 below and describes the reaction rate in terms of the initial aqueous enzyme concentration, $c_{E_0}^{aq}$, and the substrate concentration in the aqueous phase, c_A^{aq} . The

expression is also dependent on the Michaelis constant, K_m , and the turnover number, k_{cat} , which are both constants unique to each system and need to be determined experimentally.

$$r_A = \frac{k_{cat} \cdot c_A^{aq}}{K_m + c_A^{aq}} \cdot c_{E_0}^{aq} \quad (2)$$

The Michaelis-Menten equation describes an ideal situation with no inhibition of the enzyme due to other components in the system. However, as has been previously discussed, CYP153A6 is potentially inhibited by the alcohol product as well as glucose and even the alkane substrate. Therefore, the Michaelis-Menten model has been adapted to take into account various types of reversible inhibition. In reversible inhibition (which includes competitive, noncompetitive and uncompetitive inhibition) the enzyme's activity is restored when the inhibitor is removed from the system (Bhagavan & Ha, 2011). Competitive inhibition is defined as the binding of the inhibitor to the active site of the enzyme, implying that the inhibitor competes with the substrate for the active site. This inhibition can be overcome by increasing the concentration of the substrate in the system. The modified Michaelis-Menten equation, taking competitive inhibition into account, is seen in Equation 3 below (Bhagavan & Ha, 2011).

$$r_A = \frac{k_{cat} \cdot c_A^{aq}}{K_m \left(1 + \frac{c_I^{aq}}{K_i}\right) + c_A^{aq}} \cdot c_{E_0}^{aq} \quad (3)$$

Noncompetitive inhibition occurs when the inhibitor binds to the enzyme in a location distinct from the active site, inactivating the biocatalyst and indicating that the inhibition cannot be overcome by increasing the substrate concentration (Bhagavan & Ha, 2011). The modified Michaelis-Menten equation is shown below.

$$r_A = \frac{k_{cat} \cdot c_A^{aq}}{(K_m + c_A^{aq}) \left(1 + \frac{c_I^{aq}}{K_i}\right)} \cdot c_{E_0}^{aq} \quad (4)$$

The final model of reversible inhibition is uncompetitive inhibition, in which the inhibitor only binds to the enzyme-substrate complex thereby inactivating it. However, this type of inhibition is rarely observed for single-substrate systems (Bhagavan & Ha, 2011). The associated modified Michaelis-Menten equation for uncompetitive inhibition is seen in Equation 5 below.

$$r_A = \frac{k_{cat} \cdot c_A^{aq}}{K_m + c_A^{aq} \left(1 + \frac{c_I^{aq}}{K_i}\right)} \cdot c_{E_0}^{aq} \quad (5)$$

There is clearly great potential in understanding the mechanism of the hydroxylation of alkanes to primary alcohols using CYP153s. However, it is important to note that this reaction in isolation is ineffective in utilising the large source of alkanes as the biocatalyst is only able to partially convert the substrate and the alcohols produced are lower in value than the alkanes reacted. For this reason, there is a requirement for the valorisation of the alcohols into a more profitable final product.

2.2. Alcohol oxidation

Aldehydes are high-value chemicals which are used as components or intermediates in fine chemical synthesis. Hence, the oxidation of primary alcohols to aldehydes is an important process (Deplanche et al., 2011). Alcohols are historically oxidised using organic or inorganic oxidants. These methods of alcohol oxidation are environmentally and economically problematic due to the large number of by-products generated by these processes. Therefore, alcohols are rather oxidised to their corresponding aldehyde using molecular oxygen over a supported metal catalyst (Dimitratos et al., 2006).

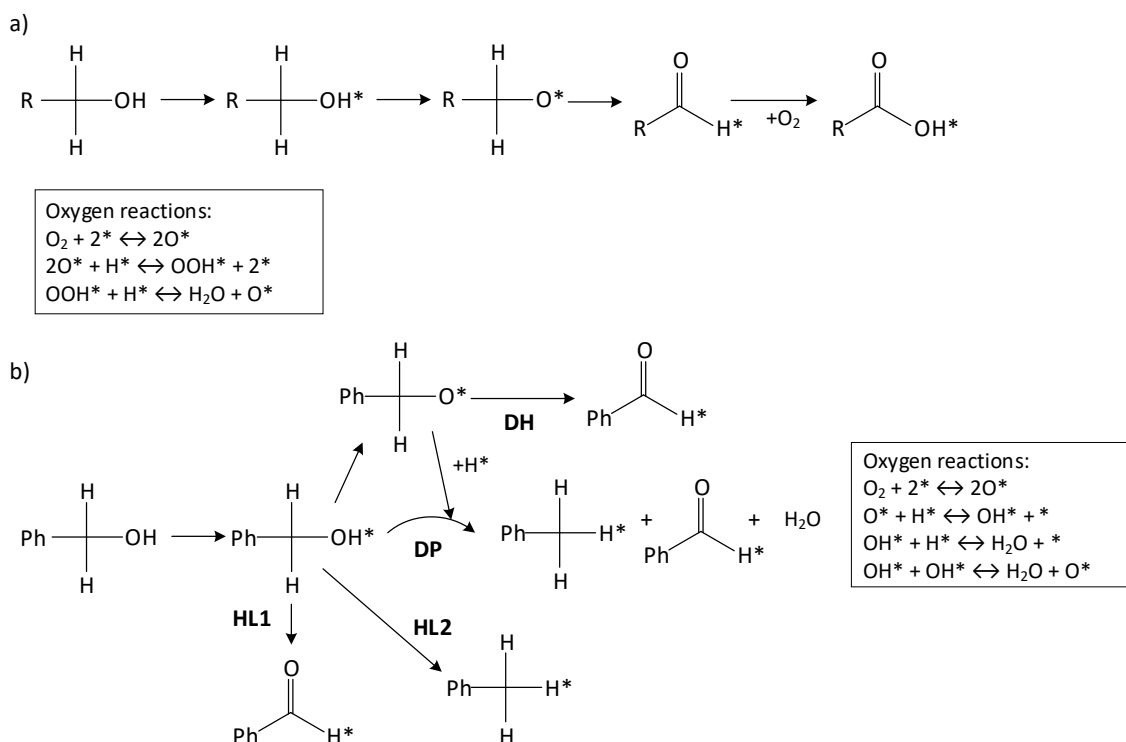


Figure 4: Reaction mechanism for the oxidation of alcohols presented by a) (Davis et al., 2013) and b) (Galvanin et al., 2018).

Over a metal catalyst, the oxidation of a primary alcohol to an aldehyde may proceed in four mechanistic steps, as shown in Figure 4a above. First, the alcohol is adsorbed onto the metal catalyst forming a metal alkoxide on the catalyst surface. A β -hydride elimination occurs on the metal alkoxide yielding an aldehyde and a metal-hydride. The final step in the mechanism is the oxidation of the metal-hydride produced by the β -hydride elimination (Davis et al., 2013). The oxidation of the metal-hydride regenerates the metal surface and forms water and oxygen. Under basic conditions, the aldehyde is reversibly hydrated to form a geminal diol. The

geminal diol then adsorbs onto the metal surface forming a metal alkoxide which undergoes a β -hydride elimination resulting in the formation of a carboxylic acid (Davis et al., 2013).

Galvanin et al. (2018) compared three models, which differ by the reaction mechanism, for the oxidation of benzyl alcohol over a synthetically supported Pd/Au catalyst. The model which best represented the observations of the experimental conversion of benzyl alcohol to benzaldehyde has a mechanism which begins with the adsorption of the alcohol onto the metal surface resulting in the formation of an adsorbed metal alkoxide and is outlined in Figure 4b. This is followed by the dehydrogenation (DH) and disproportionation (DP) of the metal alkoxide and two hydrogenolysis steps (HL1 & HL2) forming the corresponding aldehyde and alkane by-product on the metal surface. The fed oxygen dissociatively adsorbs onto the metal catalyst and is used to produce water on the metal surface (Galvanin et al., 2018). The final step in the mechanism is the desorption of the reaction products. DH, DP, HL1 and HL2 are competing reactions and are therefore assumed to be rate limiting (Galvanin et al., 2018).

Since the oxidation of alcohols is completed using a heterogeneous catalyst, a full microkinetic model can be developed using a Langmuir-Hinshelwood approach (Galvanin et al., 2018). The basis of a Langmuir-Hinshelwood kinetic model is that the first step in the reaction mechanism is the adsorption of the substrates onto the metal surface. This is followed by the chemical reaction on the metal surface with the final products desorbing from the metal surface. Therefore, the kinetic model developed is highly dependent on the reaction mechanism and rate limiting steps used (Galvanin et al., 2018). Thus, the reaction mechanisms explained by Davis et al. (2013) and Galvanin et al. (2018) would result in different microkinetic models developed using a Langmuir-Hinshelwood approach.

Multiple homogeneous and heterogeneous catalysts have been investigated for the oxidation of primary alcohols using molecular oxygen. Supported gold (Au), platinum (Pt) and palladium (Pd) chemocatalysts have shown high activity for the oxidation of alcohols (Dimitratos et al., 2006). The rate of oxidation of primary alcohols is high at temperatures between 22°C and 60°C and is dependent on the solvent in which the reaction occurs. Dimitratos et al. (2006) explain that catalyst activity is higher when water or a basic solvent is used because it facilitates the deprotonation of the alcohol. Although the use of a basic solvent increases catalyst activity, it decreases the catalyst selectivity to the aldehyde because a basic environment promotes carboxylic acid formation (Dimitratos et al., 2006). Specifically when the substrate is an aliphatic alcohol, the selectivity to the aldehyde is significantly higher in organic solvents compared to aqueous ones.

Monometallic carbon supported Au catalysts show both low conversion and selectivity. Dimitratos et al. (2006) suggest that the low activity of Au catalysts is due to their inability to remove a hydrogen from the alcohol to form a metal alkoxide. Au catalysts are highly resistant to poisoning by over oxidation and therefore have a longer lifetime. Pd and Pt monometallic systems are more active than Au catalysts but suffer significantly from oxygen poisoning (Dimitratos et al., 2006). The addition of Au to Pd and Pt catalysts improves catalyst activity by reducing the oxygen coverage on Pd and Pt catalysts. The formation of bimetallic Au-Pd and Au-Pt catalysts changes the electronic structure of the catalyst. Hence, the increased activity of bimetallic catalysts is attributed to bifunctional Au-Pd and Au-Pt active sites. The electronic interactions between components and the geometric effect due to lattice changes

in bimetallic systems are cooperative for Au-Pd and uncooperative Au-Pt systems. Hence, Au-Pd catalysts are more active than Au-Pt catalysts (Dimitratos et al., 2006).

Certain strains of bacteria are able to precipitate precious metal (Au, Pd, Pt) ions from pure solutions forming catalytically active mixtures (Deplanche et al., 2011). *E. coli* and *Desulfovibrio desulfuricans* (*D. desulfuricans*) are bacterial strains capable of reducing Pd(II) to form metallic nanoparticles (NPs) in the bacterial periplasmic space, which are catalytically active for the oxidation of primary alcohols (Creamer et al., 2007). This immobilisation of metallic NPs forms a highly reactive catalyst with a high surface area on bacterial cells that are recoverable by gravity separation (Bennett et al., 2013). These bio-supported catalysts offer a more economically and environmentally favourable route to supported Pd NPs because the bacterial support is non-toxic, and the precious metals can be obtained from secondary sources (Bennett et al., 2013).

Deplanche et al. (2011) investigates the catalytic activity of biomass supported Pd NPs combined with Au forming a Pd/Au bimetallic bionanocatalyst for the oxidation of benzyl alcohol. Bioinorganic Pd (bioPd) and bioinorganic Au (bioAu) monometallic catalysts displayed lower conversion and selectivity than the bimetallic Pd/Au bionanocatalyst. This emphasises the synergistic effect between Au and Pd when Au is added to bioPd. There are mass transfer limitations concerning the Pd/Au bionanocatalyst due to some Pd NPs not being accessible to substrates. This is attributed to the fact that some of the Pd NPs are held below the outermost layers of the bacterial surface (Creamer et al., 2007). The activity and selectivity of the Au/Pd bionanocatalyst is not impacted by the bacterial strain (*E. coli* or *D. desulfuricans*) used to reduce precious metals to form the bio-supported nanoparticles (Deplanche et al., 2011). However, the ratio of Au to Pd in the bionanocatalyst influences the catalytic activity of the bimetallic catalyst. Bimetallic catalysts which have a larger proportion of Au compared to Pd showed lower activity and selectivity than Pd catalyst doped with a small amount of Au (Deplanche et al., 2011).

Deplanche et al. (2011) compares the activity of biomass supported Pd/Au catalysts with that of a commercially available carbon supported Pd catalyst, in the absence of any solvent, for the oxidation of benzyl alcohol. The conversions achieved by both catalysts were similar, however the biomass supported catalysts were found to be more selective to the aldehyde (Deplanche et al., 2011). The activity of synthetically supported Pd/Au catalysts is investigated for the oxidation of benzyl alcohol by Dimitratos et al. (2006) in aqueous and organic solvents. The conversion achieved by the synthetic bimetallic catalysts is significantly larger than that of the bio-supported catalysts. The synthetically supported catalysts were investigated in an aqueous solvent, which increases catalyst activity (Davis et al., 2013). However, the conversion achieved by the synthetically supported catalysts is almost three times the conversion achieved by the bio-supported catalysts. Therefore, the synthetically supported catalysts would outperform the bio-supported catalysts, in terms of conversion, under the same solvent conditions (Dimitratos et al., 2006). The selectivity to the aldehyde is considerably higher when using bio-supported catalysts. Hence, the use of the bionanocatalyst favours the production of fine chemicals (Deplanche et al., 2011).

Deactivation of the catalyst used for the oxidation of primary alcohols is economically unfavourable because precious metals are expensive. Hence, improving the stability and longevity of the catalyst is highly beneficial. Therefore, the modes of deactivation must be

identified (Davis et al., 2013). Deactivation of Pd and Pt based catalysts can be rapid and can be caused by over oxidation of the metal. Au catalysts are known to be resistant to over oxidation, since it is a noble metal, but can be inhibited by the adsorption of products and by-products (Davis et al., 2013). The rate of oxidation is dependent on the rate of transfer of O₂ from the gaseous phase to the liquid phase and finally to the catalyst pores. Since the solubility of O₂ in aqueous solutions is low, the amount of catalyst loaded must be low to ensure there is sufficient mass transfer of O₂ from the gaseous phase to the liquid phase (Davis et al., 2013).

There is significant evidence of the understanding of the mechanism by which primary alcohols are oxidised to aldehydes over a metal catalyst. The ability of CYP153 monooxygenases to hydroxylate alkanes to primary alcohols has been previously outlined. The natural next step would be to complement this biotransformation by further oxidation of the alcohol to the corresponding aldehyde in one process.

2.3. Orthogonal tandem catalyst

Processes that contain multiple reaction steps are classically completed such that each reaction takes place in an individual reactor with a work-up stage in between. The main advantage of this approach is that each individual reaction can be performed at its optimal operating conditions, maximising product yields. However, this classical approach to processes with multiple reactions can be resource and time exhaustive (Gröger & Hummel, 2014). Performing multiple reactions in a single reactor is economically attractive because it utilises energy, materials and time more efficiently than multiple reactor systems (Lohr & Marks, 2015).

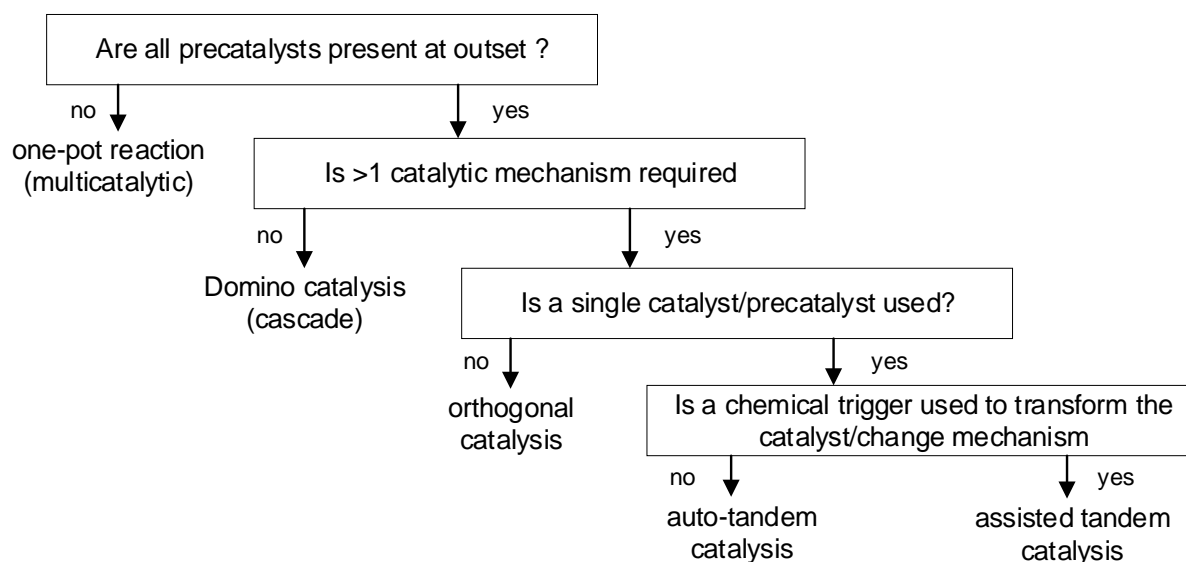


Figure 5: Classification of one-pot processes including multiple catalytic transformations (Fogg & Santos, 2004).

There are various types of one-pot reaction systems which have different reaction mechanisms, as shown in Figure 5 above. Orthogonal tandem catalysis is a one-pot system

in which multiple catalytic cycles occur sequentially and all catalysts are present from the outset of the reaction. It involves two or more functionally different and non-interfering catalysts and can be applied to complex chemical synthesis problems (Lohr & Marks, 2015). However, orthogonal tandem systems can be limited by inefficient catalyst utilisation, negative catalyst interactions and the possibility of operating at conditions which are not optimal for the reactions in the system (Fogg & Santos, 2004).

Catalyst incompatibility is often an issue in orthogonal tandem systems due to catalyst interactions especially for one-pot systems which make use of biocatalysts (enzymes) and chemocatalysts (Lohr & Marks, 2015). Huang et al. (2014) describe a method of preventing negative catalyst interactions between an enzyme and a metal catalyst by creating a compartmentalised tandem system. This is done by immobilising the enzyme on a support material, which reduces the number of interactions between the enzyme and the chemocatalyst (Huang et al., 2014). If homogenous catalysts are used, a compartmentalised tandem system can be created by placing a physical barrier between the catalysts and only allowing the relevant substrates and products to cross the barrier (Lohr & Marks, 2015). A major advantage of tandem catalysis is the ability to develop thermodynamically favourable systems. The coupling of an endothermic reaction with an exothermic reaction forms a thermodynamically favourable system driving the formation of products (Lohr & Marks, 2015).

A key opportunity in one-pot processes is the combination of biocatalytic and chemocatalytic processes. This is because these tandem reactions offer the versatility of chemocatalytic processes with the high selectivity and mild conditions shown by the enzymes used as biocatalysts (Grabner et al., 2020). Hence, the combination of the biocatalysed hydroxylation of alkanes and the oxidation of the produced alcohols over a metal catalyst to form aldehydes is an attractive prospect. The solvent in which this tandem reaction occurs strongly impacts the output of the one-pot process (Gröger & Hummel, 2014). Water is an appealing solvent to use for the tandem system combining the hydroxylation of alkanes and the oxidation of alcohols for various reasons. Firstly, water is non-toxic, environmentally friendly and cheaply available. Water is the natural reaction medium for enzymes and water (or mildly basic solvents) increases the activity of the metal nanoparticle catalyst used for the oxidation of alcohols (Gröger & Hummel, 2014).

As previously explained, CYP153 monooxygenases are capable of selectively hydroxylating alkanes to their primary alcohols. A major factor impacting the rate of hydroxylation is the substrate and product mass transfer. These alcohols are less valuable than the starting alkanes and require further valorisation. This can be done by the oxidation of primary alcohols to the corresponding aldehyde over a Pd/Au bimetallic catalyst. Bio-supported metal catalysts are more selective to the aldehyde compared to synthetically supported catalysts. The combination of the bio-hydroxylation of alkanes with the oxidation of alcohols in one-pot forms a chemoenzymatic orthogonal tandem system which is potentially less resource exhaustive than a two-pot system. The use of the highly selective CYP153 monooxygenase and bio-fabricated Pd/Au catalysts in one-system forms a process favouring the production of high purity aldehydes at lower conversion.

2.4. Objectives

The objective of this study is to investigate the kinetics of both steps to determine their relationship and the process feasibility of a one-pot system. Choosing and testing relevant hypotheses is essential in completing the goals outlined at the beginning of this research project. The two hypotheses and their motivations were therefore decided upon keeping this principle in mind and any information gained through the literature review.

2.5. Hypotheses

The first hypothesis is that alkane activation is limited by the mass transfer of the substrate from the organic phase to the aqueous phase. The rationale behind this hypothesis is that the rate of mass transfer from the organic to aqueous phases is lower than the reaction rate. The second hypothesis is that the bio-chemo tandem one-pot system is viable. The motivation for hypothesising this is despite the flexibility of the two-pot process in allowing disparate reaction conditions, the one-pot process will achieve a sufficient conversion to the aldehyde for the coupling of the two separate reaction steps to be feasible. The answer to whether these hypotheses have been proven or disproven will provide a great deal of insight into the future potential of the orthogonal bio-chemo tandem system in activating alkanes to aldehydes.

2.6. Key questions

To successfully achieve the objectives set out at the initiation of this project, it is necessary to focus the investigation towards answering certain key questions. These questions will guide the decision making throughout the project and will enable testing of the hypotheses which have been proposed. The key questions which have been decided upon are as follows:

- What inhibits the alkane activation reaction in the one-pot system?
- What impact does the enzyme inhibition have on process variables?
- What is the optimal reactor configuration for the upgrading of alkanes to aldehydes?

By answering these questions, a better understanding will be gained of the bio-chemo tandem process and the feasibility of competing the two reactions in a one-pot system.

3. RESEARCH APPROACH AND MODEL DEVELOPMENT

3.1. Methodology

The research approach for this study can be broken down into three distinct parts. The first phase of the study is the kinetic model development for the biotransformation of octane and the chemocatalysed oxidation of 1-octanol. These kinetic models are then applied to two-pot and one-pot reactor systems in order to understand the behaviour of both. The final stage of the study is to compare both the one and two-pot systems and to determine their potential feasibility on an economic basis. Figure 6 below shows the detailed methodology used to test the hypotheses and answer the key questions previously outlined.

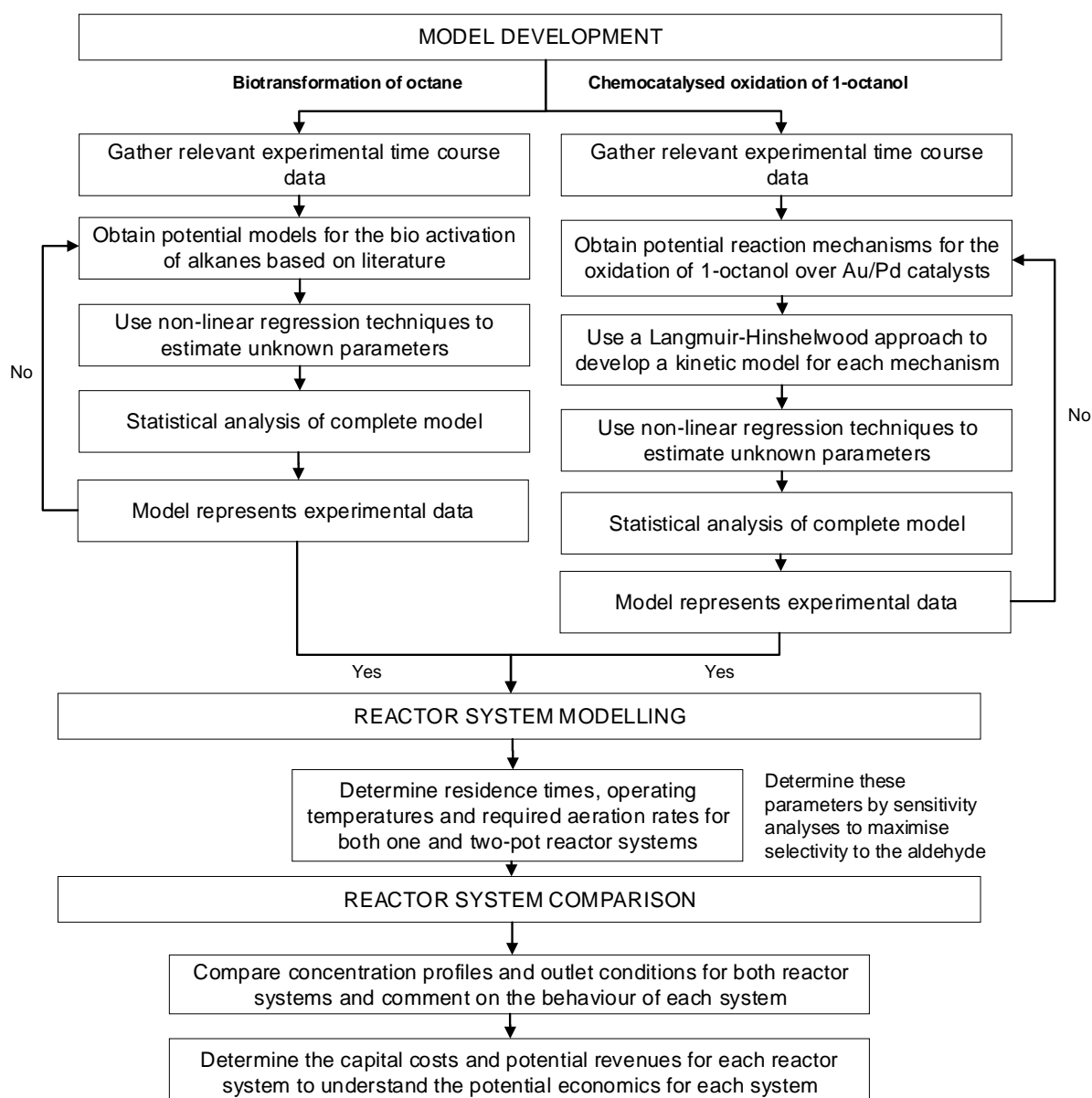


Figure 6: Research method used in the study

3.2. Alkane activation kinetic model development

3.2.1. Data sourcing

No laboratory experimental work was done during the undertaking of this research project and thus the data necessary to analyse the alkane hydroxylation reaction needed to be obtained from external sources. The Centre for Bioprocess Engineering Research (CeBER) at the University of Cape Town provided data for different experimental procedures, each measuring the change in concentration of octanol over time when an octane substrate was provided to the CYP153A6 biocatalyst. The full experimental procedure can be found in Appendix A, along with the raw concentration data obtained. Of the various procedures described, the data set used for any further modelling was chosen by selecting the results which had the highest initial enzyme activity while maximising the amount of octanol produced, seen as procedure 2c as described in Appendix A.

The initial octane concentration was determined by considering the volume of substrate added to the experimental vial. Because 0.1 mL of octane was added to a 1.3 mL reaction volume, also containing 0.1 mL of bis(2-ethylhexyl)phthalate (BEHP) and 1 mL of cell suspension, the initial substrate concentration was calculated to be 946.8 mmol/L, providing an excess of octane to prevent the substrate concentration from limiting the reaction.

3.2.2. Potential reaction mechanisms

As was laid out in the literature review, the consumption of substrate by the biocatalyst within the hydroxylation of the alkane can be described by a few different potential mechanisms. The Michaelis-Menten equation (Equation 2) relates the rate of the reaction to the concentrations of both the enzyme and the substrate present. This equation describes many biocatalysed reactions and thus could potentially describe the activation of octane to alcohol through the use of CYP153A6. However, the biphasic nature of this system (the enzyme present in the aqueous phase with the substrate present in the organic phase) means that other mechanisms could potentially also play a role in the alkane hydroxylation. The mass transfer and interfacial adsorption models were described in the literature review section of the report and their mechanisms can be seen in Figure 3.

The mass transfer model adapts the initial Michaelis-Menten equation by inserting additional parameters which better describe what is taking place within the system. This model is based on the assumption that the rate of the reaction is equal to the rate of transfer of the alkane from the organic phase to the aqueous phase (Straathof, 2003). This relationship can be seen further in Equation 6 below, noting that the concentration of the organic substrate in the aqueous phase, c_A^{aq} , is low and difficult to measure and that the octanol concentration presented in the data is located in the organic phase. Therefore, it is necessary to rearrange Equation 6 to eliminate this unknown concentration and use this expression for the aqueous substrate concentration within the Michaelis-Menten equation to determine the reaction rate as discussed previously.

$$k_L a \cdot \left(\frac{c_A^{org}}{m} - c_A^{aq} \right) = \frac{k_{cat} \cdot c_A^{aq}}{K_m + c_A^{aq}} \cdot c_{E_0}^{aq} \quad (6)$$

The rearrangement of Equation 6 can be found in Equation 7 below (Straathof, 2003).

$$c_A^{aq} = \frac{-b_1 + \sqrt{(b_1)^2 + 4K_m \cdot \frac{c_A^{org}}{m}}}{2} \quad (7)$$

Where the term b_1 is explained further in Equation 8 below.

$$b_1 = \frac{k_{cat} \cdot c_{E_0}^{aq}}{k_L a} + K_m - \frac{c_A^{org}}{m} \quad (8)$$

The expression to describe the aqueous substrate concentration, Equations 7 and 8, can therefore be substituted into Equation 2 to create a full model to describe any potential mass transfer limitations within the system. In addition to the system constants described in the literature review for the Michaelis-Menten equation, k_{cat} and K_m , there are other constants which are included as part of the mass transfer model. The partition coefficient, m , describes the distribution of the substrate within the two phases, while $k_L a$ refers to the volumetric mass transfer coefficient between the biphasic system where a in particular describes the volume-specific interfacial area (Straathof, 2003).

The mechanism described by the interfacial adsorption model can be seen in Equation 9 below and relates the reaction rate to the amount of enzyme adsorbed per m^2 of interface, Γ (Straathof, 2003). As with the aqueous substrate concentration in the mass transfer model, the amount of enzyme adsorbed on the interface is difficult to measure and therefore additional equations are necessary to describe it in order for it to be incorporated within the model.

$$r_A = \frac{k_{cat} \cdot c_A^{org}}{K_m + c_A^{org}} \cdot \Gamma \cdot a \quad (9)$$

The assumption used to develop an expression for the interfacial enzyme concentration is that the system obeys Langmuir adsorption and thus Γ can be described by Equation 10 below (Straathof, 2003).

$$\Gamma = \frac{\Gamma_{max} \cdot c_E^{aq}}{\frac{1}{K} + c_E^{aq}} \quad (10)$$

The saturation enzyme concentration at the interface is represented by Γ_{max} while K describes the Langmuir adsorption constant (Straathof, 2003). The enzyme concentration in the aqueous phase, c_E^{aq} , will be different from the known initial enzyme concentration discussed previously, $c_{E_0}^{aq}$, and thus a further relation which can be seen in below in Equation 11 is

needed to relate these two quantities by considering the size of the interfacial area, A , and the volume of the aqueous phase V^{aq} (Straathof, 2003).

$$V^{aq} \cdot c_{E_0}^{aq} = V^{aq} \cdot c_E^{aq} + \Gamma \cdot A \quad (11)$$

Because a certain amount of enzyme has been adsorbed onto the interface, the concentration remaining in the aqueous phase is simply equal to the difference between the initial concentration and the amount adsorbed, as shown in Equation 11. Therefore, an expression for this unknown concentration of enzyme in the aqueous phase can be substituted back into Equation 10. This substitution can be seen in more detail in Equation 12.

$$\Gamma = \frac{\Gamma_{max} \cdot (c_{E_0}^{aq} - \Gamma \cdot a)}{\frac{1}{K} + (c_{E_0}^{aq} - \Gamma \cdot a)} \quad (12)$$

Therefore, this relationship can be written purely in terms of the interfacial enzyme concentration and is therefore substituted into Equation 9, describing the rate of the reaction for the interfacial adsorption model. The final rate equation can be found in Equation 13 with the term b_2 being described further below.

$$r_A = \frac{k_{cat} \cdot c_A^{org}}{K_m + c_A^{org}} \cdot \frac{b_2 - \sqrt{(b_2)^2 - 4\Gamma_{max} \cdot a \cdot c_{E_0}^{aq}}}{2} \quad (13)$$

$$b_2 = \Gamma_{max} \cdot a + \frac{1}{K} - c_{E_0}^{aq} \quad (14)$$

Ultimately, the Michaelis-Menten (MM), mass transfer (MT) and interfacial adsorption (IA) models all need to be compared to the experimental data. The parameters within each model need to be regressed to determine which of them best describes the reaction.

3.3. Alcohol oxidation kinetic model development

3.3.1. Data sourcing

Similarly to the development of the alkane activation model, no laboratory work was completed within the duration of the project. However, there is still a requirement for concentration-time profiles for the oxidation of primary alcohols over a Pd/Au catalyst in order to develop a kinetic model of the reaction. The time-course data for this reaction was sourced from Villa et al. (2009) which measures the conversion of 1-octanol as a function of time. This data was measured using an initial 1-octanol concentration of 0.3 M which was used to convert the conversion-time data into a concentration-time profile (Villa et al., 2009). The full experimental procedure, along with the raw data, can be found in Appendix A.

The catalyst used by Villa et al. (2009) to obtain the required concentration-time data, is an activated carbon supported Pd₈₀/Au₂₀ catalyst. This catalyst is assumed to behave similarly to a bio-supported Pd/Au catalyst due to the lack of experimental time-course data for the oxidation of 1-octanol over a bio-supported Pd/Au catalyst. Thus, it is assumed that the kinetic model developed for the synthetically supported Pd/Au catalysts sufficiently models the behaviour of the bio-supported catalyst.

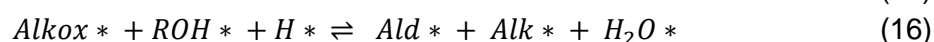
3.3.2. Potential reaction mechanisms

In order to develop a full kinetic model for the chemocatalysed oxidation of 1-octanol, using a Langmuir-Hinshelwood approach, a chemically consistent reaction mechanism is required. The reaction mechanism is developed using an understanding of the main reaction species present on the catalyst surface (Galvanin et al., 2018). For this study, two kinetic models based on different mechanisms were developed and compared to determine which one best fits the experimental data.

3.3.2.1. Reaction mechanism for Model 0

The mechanism used by Model 0 assumes the oxidation of 1-octanol over a gold-palladium catalyst follows a similar reaction mechanism to that of benzyl alcohol since it is often used to model alcohol oxidation in catalytic tests (Davis et al., 2013). The first step in this mechanism is the adsorption of the alcohol substrate onto the catalyst surface. The active sites of the catalyst then remove the hydrogen from the hydroxyl group to form an adsorbed metal alkoxide and metal hydride.

In order to describe the product formation, the mechanism contains four competitive reactions which form the desired aldehyde (octanal) and corresponding alkane (octane) from the alcohol substrate. These competitive reactions are a dehydrogenation reaction (DH), disproportionation reaction (DP) and two hydrogenolysis reactions (HL1 and HL2) and are shown in Equations 15, 16, 17 and 18 respectively (Galvanin et al., 2018).



Oxygen is assumed to adsorb dissociatively on the catalyst surface and reacts with the surface bound metal hydride to regenerate it and directly form water as seen in Table 1 (Galvanin et al., 2018). It is important to note that in this model, oxygen does not interact with the alcohol substrate with its primary function being to regenerate the catalyst surface. The final step in the reaction is the desorption of the aldehyde and alkane products from the catalyst surface.

3.3.2.2. Reaction mechanism for Model 1

According to Davis et al. (2013), the oxidation of a primary alcohol initially forms an aldehyde which can be subsequently oxidised to a carboxylic acid. Similar, to the mechanism shown for Model 0, the first step is the chemisorption of the alcohol substrate onto the catalyst. The hydrogen from the hydroxyl group is subsequently removed by the active sites to form an adsorbed metal alkoxide and metal hydride. The metal alkoxide is then known to undergo a

β -hydride elimination to form an adsorbed aldehyde which is further oxidised to the corresponding carboxylic acid, as shown in Equations 19 and 20 respectively. These reactions are assumed to be competitive reactions and are thus rate limiting.



Dissociatively adsorbed oxygen reacts with the previously formed metal hydride species to produce water through a peroxide intermediate, as shown in Table 2. As in Model 0, oxygen is responsible for the regeneration of the catalyst surface, but it also directly interacts with the aldehyde to form the carboxylic acid. Therefore, the concentration of oxygen within the system impacts the selectivity to the aldehyde product.

3.3.3. Formulation of kinetic models

In order to develop a full microkinetic expression for each of the aforementioned mechanisms, a Langmuir-Hinshelwood approach is used. For both models it was assumed that the adsorption and desorption of reactants and products were very fast and thus the system was assumed to be limited by the reaction rate of the rate limiting steps. Furthermore, it is assumed that there is constant surface coverage (θ_*) on the catalyst.

3.3.3.1. Development of Model 0

The full reaction mechanism along with the equilibrium expression for each reaction for Model 0 is shown in Table 1 below. The equilibrium expressions are developed assuming that the rate order of each component is equivalent to stoichiometric coefficient of that component in each reaction as a result of using a Langmuir-Hinshelwood approach.

Table 1: Full reaction mechanism for Model 0 along with equilibrium equation for each reaction with the rate limiting steps shown in bold (Galvanin et al., 2018).

| Reaction | Equilibrium equation |
|---|--|
| 1. $\text{ROH} + * \rightleftharpoons \text{ROH}^*$ | $\theta_{\text{ROH}^*} = K_1[\text{ROH}]\theta_*$ |
| 2. $\text{ROH}^* + * \rightleftharpoons \text{Alkox}^* + \text{H}^*$ | $\theta_{\text{Alkox}^*} = K_2\theta_{\text{ROH}^*}\theta_*/\theta_{\text{H}^*}$ |
| 3. $\text{Alkox}^* + * \rightleftharpoons \text{Ald}^* + \text{H}^*$ | $r_3 = k_3\theta_{\text{Alkox}^*}\theta_* - k_{-3}\theta_{\text{Ald}^*}\theta_{\text{H}^*}$ |
| 4. $\text{Alkox}^* + \text{ROH}^* + \text{H}^* \rightleftharpoons \text{Ald}^* + \text{Alk}^* + \text{H}_2\text{O}^*$ | $r_4 = k_4\theta_{\text{Alkox}^*}\theta_{\text{ROH}^*}\theta_{\text{H}^*} - k_{-4}\theta_{\text{Ald}^*}\theta_{\text{Alk}^*}\theta_{\text{H}_2\text{O}^*}$ |
| 5. $\text{ROH}^* + \text{H}^* \rightleftharpoons \text{Alk}^* + \text{OH}^*$ | $r_5 = k_5\theta_{\text{ROH}^*}\theta_{\text{H}^*} - k_{-5}\theta_{\text{Alk}^*}\theta_{\text{OH}^*}$ |
| 6. $\text{ROH}^* + 2* \rightleftharpoons \text{Ald}^* + 2\text{H}^*$ | $r_6 = k_6\theta_{\text{ROH}^*}\theta_*^2 - k_{-6}\theta_{\text{Ald}^*}\theta_{\text{H}^*}^2$ |
| 7. $\text{O}_2 + 2* \rightleftharpoons 2\text{O}^*$ | $\theta_{\text{O}^*} = K_7[\text{O}_2]^{1/2}\theta_*$ |
| 8. $\text{O}^* + \text{H}^* \rightleftharpoons \text{OH}^* + *$ | $\theta_{\text{OH}^*} = K_8\theta_{\text{O}^*}\theta_{\text{H}^*}/\theta_*$ |
| 9. $\text{OH}^* + \text{H}^* \rightleftharpoons \text{H}_2\text{O}^* + *$ | $\theta_{\text{H}_2\text{O}^*} = K_9\theta_{\text{OH}^*}\theta_{\text{H}^*}/\theta_*$ |
| 10. $\text{OH}^* + \text{OH}^* \rightleftharpoons \text{H}_2\text{O}^* + \text{O}^*$ | $\theta_{\text{H}_2\text{O}^*} = K_{10}\theta_{\text{OH}^*}^2/\theta_*$ |
| 11. $\text{Alk}^* \rightleftharpoons \text{Alk} + *$ | $\theta_{\text{Alk}^*} = [\text{Alk}]\theta_*/K_{11}$ |
| 12. $\text{Ald}^* \rightleftharpoons \text{Ald} + *$ | $\theta_{\text{Ald}^*} = [\text{Ald}]\theta_*/K_{12}$ |
| 13. $\text{H}_2\text{O}^* \rightleftharpoons \text{H}_2\text{O} + *$ | $\theta_{\text{H}_2\text{O}^*} = [\text{H}_2\text{O}]\theta_*/K_{13}$ |

θ_{i^*} - indicates the concentration of species i on the catalyst surface

$*$ - represents an active site on the catalyst surface

Using the equilibrium equations shown in Table 1, the coverage of each reaction species on the catalyst surface can be related to the bulk concentrations of each component, as shown in Equations 21 to 28 (Galvanin et al., 2018).

$$\theta_{ROH*} = K_1[ROH]\theta_* \quad (21)$$

$$\theta_{O*} = K_7[O_2]^{1/2}\theta_* \quad (22)$$

$$\theta_{Alkox*} = K_1K_2\sqrt{K_7K_8K_9K_{13}} \frac{[ROH][O_2]^{1/4}}{[H_2O]^{1/2}}\theta_* \quad (23)$$

$$\theta_{H*} = \frac{1}{\sqrt{K_7K_8K_9K_{13}}} \frac{[H_2O]^{1/2}}{[O_2]^{1/4}}\theta_* \quad (24)$$

$$\theta_{OH*} = \frac{\sqrt{K_7K_8K_9K_{13}}}{K_9K_{13}} [H_2O]^{1/2}[O_2]^{1/4}\theta_* \quad (25)$$

$$\theta_{Alk*} = [Alk]\theta_*/K_{11} \quad (26)$$

$$\theta_{Ald*} = [Ald]\theta_*/K_{12} \quad (27)$$

$$\theta_{H_2O*} = [H_2O]\theta_*/K_{13} \quad (28)$$

By determining the coverage of each reaction species on the catalyst species, the rate expressions of the rate limiting steps (shown in Table 1) can be computed as a function of the bulk concentration of each reaction component. By substituting the surface concentrations into the rate expressions of the rate limiting steps various constants, such as equilibrium constants (K_i) and the surface coverage (θ_*), will end up being multiplied together. Since these variables are all constants, they are lumped into a single rate constant, k_i , in order to simplify the model giving the following reaction rate expressions for the rate limiting steps (Galvanin et al., 2018).

$$r_3 = k_0 \frac{[ROH][O_2]^{1/4}}{[H_2O]^{1/2}} - k_1 \frac{[Ald][H_2O]^{1/2}}{[O_2]^{1/4}} \quad (29)$$

$$r_4 = k_2[ROH]^2 - k_3[Ald][Alk][H_2O] \quad (30)$$

$$r_5 = k_4 \frac{[ROH][H_2O]^{1/2}}{[O_2]^{1/4}} - k_5[Alk][H_2O]^{1/2}[O_2]^{1/4} \quad (31)$$

$$r_6 = k_6[ROH] - k_7 \frac{[Ald][H_2O]}{[O_2]^{1/2}} \quad (32)$$

The reaction rate expressions shown in Equations 29 to 32 make up the full microkinetic model described by Model 0.

3.3.3.2. Development of Model 1

As previously described, the full reaction mechanism for Model 1 is shown along with the equilibrium equations in Table 2 below. As a result of using a Langmuir-Hinshelwood approach, it was assumed that the rate order of each component is equivalent to the stoichiometric coefficient of that component in each reaction.

Table 2: Full reaction mechanism for Model 1 along with equilibrium equation for each reaction with the rate limiting steps shown in bold (Davis et al., 2013).

| Reaction | Equilibrium equation |
|---|---|
| 1. $ROH + * \rightleftharpoons ROH *$ | $\theta_{ROH*} = K_1[ROH]\theta_*$ |
| 2. $ROH * + * \rightleftharpoons Alkox * + H *$ | $\theta_{Alkox*} = K_2\theta_{ROH*}\theta_*/\theta_{H*}$ |
| 3. $Alkox * + * \rightleftharpoons Ald * + H *$ | $r_3 = k_3\theta_{Alkox*}\theta_* - k_{-3}\theta_{Ald*}\theta_{H*}$ |
| 4. $O_2 + 2 * \rightleftharpoons 2O *$ | $\theta_{O*} = K_4[O_2]^{1/2}\theta_*$ |
| 5. $2O * + H * \rightleftharpoons OOH * + 2 *$ | $\theta_{OOH*} = K_5\theta_{O*}^2\theta_{H*}/\theta_*^2$ |
| 6. $OOH * + H * \rightleftharpoons H_2O * + O *$ | $\theta_{H_2O*} = K_6\theta_{OOH*}\theta_{H*}/\theta_{O*}$ |
| 7. $Ald * + O * \rightleftharpoons Car * + *$ | $r_7 = k_7\theta_{Ald*}\theta_{O*} - k_{-7}\theta_{Car*}\theta_*$ |
| 8. $Ald * \rightleftharpoons Ald + *$ | $\theta_{Ald*} = [Ald]\theta_*/K_8$ |
| 9. $Car * \rightleftharpoons Car + *$ | $\theta_{Car*} = [Car]\theta_*/K_9$ |
| 10. $H_2O * \rightleftharpoons H_2O + *$ | $\theta_{H_2O*} = [H_2O]\theta_*/K_{10}$ |

θ_{i*} - indicates the concentration of species i on the catalyst surface

$*$ - represents an active site on the catalyst surface

Equations 33 to 39 show the coverage of each individual reaction species on the catalyst surface can be determined as a function of the bulk concentrations of each component. These were computed using the equilibrium expressions shown in Table 2.

$$\theta_{ROH*} = K_1[ROH]\theta_* \quad (33)$$

$$\theta_{O*} = K_4[O_2]^{1/2}\theta_* \quad (34)$$

$$\theta_{H*} = \frac{1}{\sqrt{K_4K_5K_6K_{10}}} \frac{[H_2O]^{1/2}}{[O_2]^{1/4}} \theta_* \quad (35)$$

$$\theta_{Alkox*} = K_1K_2\sqrt{K_4K_5K_6K_{10}} \frac{[ROH][O_2]^{1/4}}{[H_2O]^{1/2}} \theta_* \quad (36)$$

$$\theta_{Ald*} = [Ald]\theta_*/K_8 \quad (37)$$

$$\theta_{Car*} = [Car]\theta_*/K_9 \quad (38)$$

$$\theta_{H_2O*} = [H_2O]\theta_*/K_{10} \quad (39)$$

Using the expressions for the surface coverage of each component, the rate expressions for the rate limiting steps are also related to the bulk concentration of the reaction components. As found in Model 0, by substituting the surface coverages into the rate expressions for the rate limiting steps, various constants are multiplied together. This allows all these constants to be lumped into a single rate constant, k_i , to simplify the full model expressions shown in the equations below.

$$r_3 = k_0 \frac{[ROH][O_2]^{1/4}}{[H_2O]^{1/2}} - k_1 \frac{[Ald][H_2O]^{1/2}}{[O_2]^{1/4}} \quad (40)$$

$$r_7 = k_2[Ald][O_2]^{1/4} - k_3[Car] \quad (41)$$

3.4. Reactor modelling

The development of the mechanisms and kinetics of both the alkane activation and the alcohol oxidation enables the reactions to be modelled within a physical reactor, using its design equation. For the purposes of this research project, a continuous reactor was chosen due to the generation of an aldehyde as the final product and because continuous processes are more economical for large-scale fine chemical synthesis (Hartman, 2020).

In this manner, the feasibility of the one-pot process relative to a two-pot system can be determined for the production of aldehydes from an alkane feedstock. A continuous stirred tank reactor (CSTR) is an example of an ideal continuous reactor as it relies on the assumption that the system is perfectly mixed and that there is a uniform concentration distribution within its volume. over

The design equation of the CSTR is based on the material balance of the components taking part in the reaction, where this general mole balance can be seen in Equation 42 below. This equation relates the accumulation of a component to its inlet and outlet flowrates as well as what has been generated or consumed within the reactions.

$$\frac{dN_A}{dt} = F_{A,0} - F_A + G_A \quad (42)$$

When adapting this equation to be used in a CSTR, it can be assumed that the volumetric flowrate exiting and leaving the system are constant and that the equation can therefore be written in terms of component concentrations. This can be seen below, where the generation term has also been described using the reaction rate and the volume of the reactor.

$$\frac{VdC_A}{dt} = v(C_{A,0} - C_A) + r_A V \quad (43)$$

Dividing the entire expression by the volume allows the equation to be expressed in terms of residence time, the ratio of the reactor volume to the volumetric flowrate, seen in Equation 44.

$$\frac{dC_A}{dt} = \frac{(C_{A,0} - C_A)}{\tau} + r_A \quad (44)$$

This equation describes the change in concentration of the components over time. The CSTR initially undergoes a period of transient operation, in which the exiting concentrations change as a function of time. However, as the amount of time gets large (i.e. $t \rightarrow \infty$), the system begins to operate at steady state and the exiting concentrations become constant (Kanse Nitin, Dhanke & Thombare, 2012).

In terms of Equation 44, this situation is accounted for in the accumulation term becoming equal to zero since the system is no longer changing with time. This is what produces the traditional steady state CSTR equation seen in Equation 45.

$$\tau = \frac{(C_{A,0} - C_A)}{-r_A} \quad (45)$$

4. RESULTS AND DISCUSSION

4.1. Alkane activation kinetic modelling and parameter estimation

The nature of the three proposed models previously discussed in the potential alkane activation mechanisms section is that the unknown parameters need to be solved using non-linear regression techniques. The concentration data was obtained for a batch system converting octane to octanol thus it is necessary to relate these values to a reaction rate using a batch reactor design equation. The batch reactor equation relates the change in concentration of the substrate or product to the rate of the reaction and can be seen below.

$$\frac{dC_P}{dt} = - \frac{dC_A}{dt} = r_A \quad (46)$$

The reaction rate in Equation 46 is different for each of the models proposed as has been described in the potential mechanisms section. Therefore, the unknown parameters were determined for each model by solving the ordinary differential equation (ODE) in Equation 46 and using a Levenberg-Marquardt non-linear solver to minimise the difference between the octanol production predicted by the models and that determined experimentally. A summary of the parameters solved for each model can be seen in detail in Tables 3, 4 and 5 respectively.

Table 3: Summary of parameter estimation for Michaelis-Menten model.

| Parameter | Value |
|-------------------------------|--------|
| k_{cat} [h^{-1}] | 10.161 |
| K_m [mM] | 19.743 |

Table 4: Summary of parameter estimation for mass transfer model.

| Parameter | Value |
|-------------------------------|--------|
| k_{cat} [h^{-1}] | 15.340 |
| K_m [mM] | 19.999 |
| $k_L a$ [h^{-1}] | 24.975 |

Table 5: Summary of parameter estimation for interfacial adsorption model.

| Parameter | Value |
|-------------------------------|--------|
| k_{cat} [h^{-1}] | 13.093 |
| K_m [mM] | 19.083 |
| Γ_{max} [mM] | 0.502 |
| K [mM^{-1}] | 6.365 |

For the mass transfer model, the value for the partition coefficient was not regressed but was obtained from literature as it has a standard value of 5 for a system containing octanol and water (Olaofe et al., 2013). Once the parameters had been estimated using non-linear

regression it was necessary to compare the fully specified models to determine which of them managed to best predict the experimental data. The curves for the Michaelis-Menten, mass transfer and interfacial adsorption models can be seen in Figure 7 below.

The results presented show that the models are reasonably similar in predicting the mechanism of reacting octane to octanol using CYP153A6 as the biocatalyst but that the mass transfer mechanism most closely displays the expected trend. The high initial excess concentration of the substrate means the conversion of the substrate reaches a maximum after a long period, thus it was not possible to obtain concentration data for high conversion values. Therefore, the data is situated at low octane conversions and the accuracy of the models at higher conversions could not be determined. However, out of these models, the mass transfer mechanism was calculated to be slightly more accurate as can be seen from the statistical results presented below.

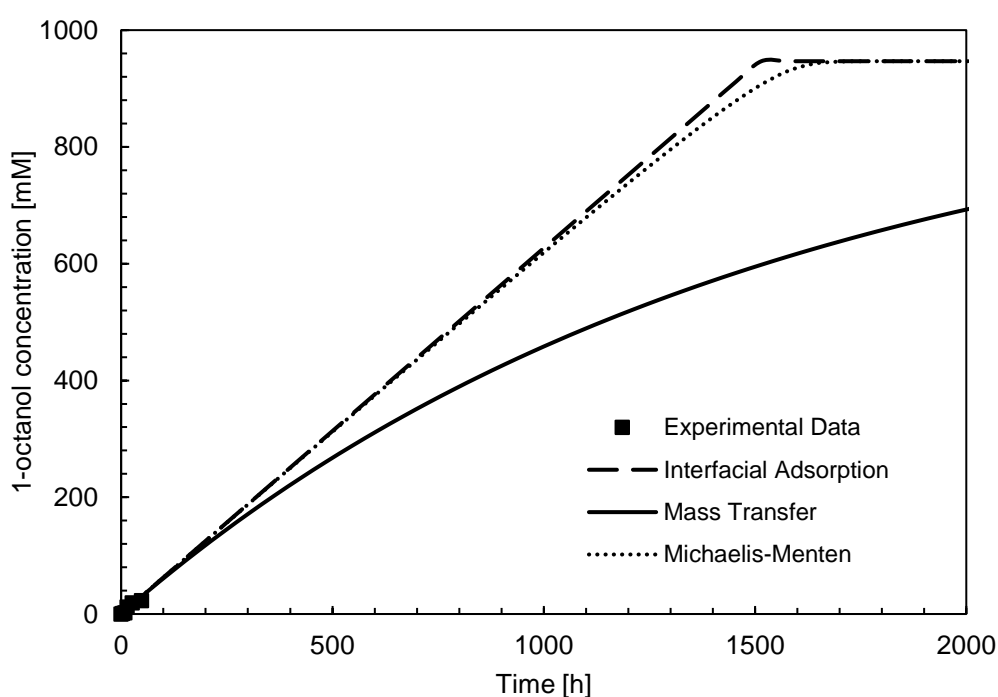


Figure 7: Comparison of proposed models for high initial substrate concentrations. Data obtained from (Centre for Bioprocess Engineering Research, 2020).

Table 6: Statistical results of proposed alkane activation models.

| Model | Pearson Correlation | χ^2 Test |
|------------------------|---------------------|---------------|
| Michaelis-Menten | 0.9530 | 2.1015 |
| Mass Transfer | 0.9718 | 1.4027 |
| Interfacial Adsorption | 0.9530 | 2.1015 |

The χ^2 test calculated in Table 6 above relates the goodness of fit of the experimental data to the results predicted by each of the proposed mechanisms. The most adequate model is

therefore the one which produces the lowest χ^2 value, leading to the conclusion that the mass transfer model best represents the system (Galvanin et al., 2018). This is supported by both the results presented in Figure 7 as well as the Pearson Correlation reported in Table 6.

When the models are used to predict octanol concentrations with a lower initial concentration of octane, it is found that again the mass transfer model best predicts the behaviour of the alkane hydroxylation system. Figure 8 below displays the results of all three models and the experimental data for a lower initial octane concentration and this curve is what further confirms that the mass transfer model is the optimal one for the given reaction and thus will be used in any further reactor modelling completed and any results obtained.

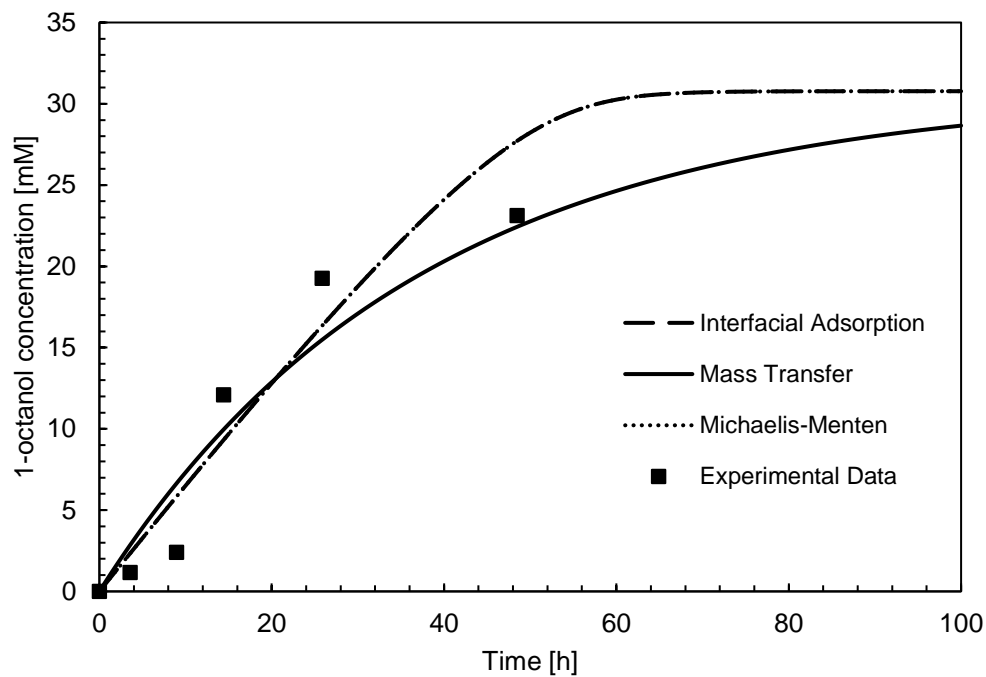


Figure 8: Comparison of proposed models for low initial substrate concentrations. Data obtained from (Centre for Bioprocess Engineering Research, 2020).

4.2. Alcohol oxidation kinetic modelling and parameter estimation

Both Models 0 and 1 discussed in the formulation of kinetic models for alcohol oxidation contain rate constants which need to be determined. These rate constants, k_i , are assumed to follow an Arrhenius relationship with temperature and are thus described by Equation 47.

$$k_i = A_i \exp\left(-\frac{Ea_i}{RT}\right) \quad (47)$$

Where R is the ideal constant with a value of 8.314 J/mol.K. By substituting this relationship for the rate constant into both models, the nature of the resulting equations shows that non-linear regression solving techniques are required to estimate the numerical values of the unknown parameters, A_i and Ea_i . Since the 1-octanol oxidation concentration-time data,

sourced from Villa et al. (2009), was produced using a batch reactor, the kinetic models need to be evaluated using the batch reactor design equation, shown in Equation 48 below, in order to relate the models to the experimental data.

$$\frac{dC_i}{dt} = v_i r_{ij} \quad (48)$$

Where v_i is the stoichiometric coefficient of component i and r_{ij} is the rate of formation or consumption of component i in reaction j . The rate of formation or consumption of each component is described using Models 0 and 1. Therefore, the unknown parameters were determined for each model by solving the ODE, shown in Equation 48, and using a Nelder-Mead non-linear solver to minimise the difference between the 1-octanol consumption predicted by the models and those determined experimentally. The Nelder-Mead algorithm was used for parameter estimation because the number of unknown parameters exceeded the number of equations for both models. A summary of the parameters solved for in each model are shown in Tables B1 and B2 in Appendix B. The orders of magnitude of the parameters estimated are in line with those found in literature (Galvanin et al., 2018).

Once the parameters for both models have been estimated using non-linear regression, the fully specified models are compared on a graphical and statistical basis to determine the model which best predicts the experimental data. Figure 9 below outlines the ability for both kinetic models to predict the experimental 1-octanol consumption data. The slow rate of reaction shown by the experimental data (and as a result by both models) can be attributed to the high proportion of Au in comparison to Pd nanoparticles in the catalyst.

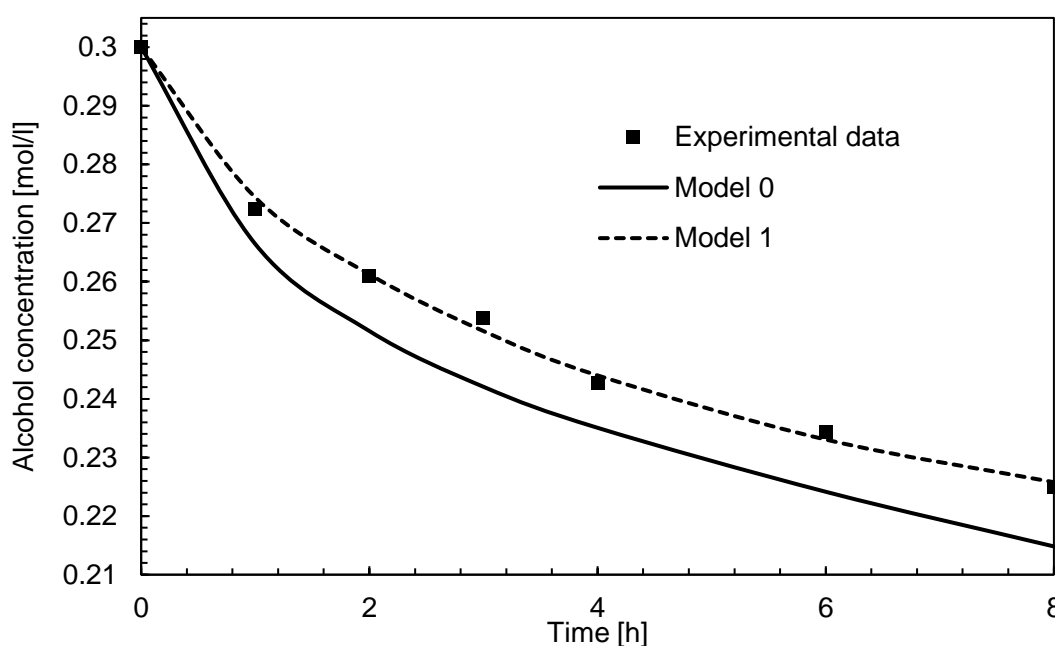


Figure 9: Comparison of proposed models for alcohol oxidation over a Pd_{80}/Au_{20} catalyst to experimental data obtained from (Villa et al., 2009).

Figure 9 suggests that Model 1 is more accurate in predicting the experimental 1-octanol experimental data. In addition to this it shows that the Model 0 overestimates the amount of 1-octanol converted over time. To ensure this claim is statistically relevant, a statistical analysis of the predicted and expected data for both models was undertaken, with the results shown in Table 7. The Pearson Correlation coefficient shows the level of association between two variables. Therefore, the high Pearson Correlation coefficients for both models, highlighted in Table 7, indicates that the relationship between alcohol concentration over time is well represented by both models, with Model 1 better predicting the trends shown by the experimental data. The more important statistical analysis to examine is the chi-square test which measures the goodness of fit for each model to the experimental data (Galvanin et al., 2018). The significantly lower chi-square test value for Model 1 compared to Model 0, indicates that Model 1 best fits the experimental data.

Table 7: Summary of statistical analysis for the comparison of the proposed models for alcohol oxidation

| Model | Pearson Correlation | χ^2 Test |
|---------|---------------------|-----------------------|
| Model 0 | 0.997 | 2.25×10^{-3} |
| Model 1 | 0.998 | 5.06×10^{-5} |

4.3. Two-pot system

Once the kinetic models for each of the subsequent steps in the activation of alkanes to aldehydes have been developed, along with a suitable reactor design equation, they can be brought together to determine the potential benefit of combining the two reactions within both one and two-pot systems. Within the two-pot system, it is necessary to model the two reaction steps separately by determining the optimal reactor operating conditions of each. Because the second step in a two-pot system is highly dependent on the feed it receives from the first, it is necessary to successfully model this initial reaction and ensure the process operates efficiently before any modelling of the subsequent alcohol oxidation. A simple representation of how this two-pot process would be configured can be seen in Figure 10 below.

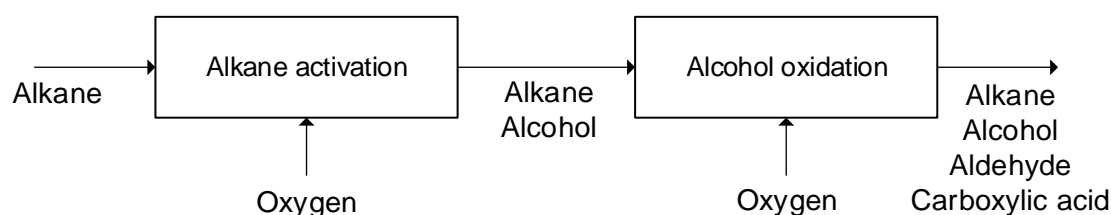


Figure 10: Simple representation of two-pot process.

The temperature of the alkane activation taking place in the first step of the sequence was maintained at 20°C due to the significant decreases in enzyme activity and alcohol production observed, as discussed in the literature review section of the report, when the temperature is increased even slightly to 25°C (Olaofe et al., 2013). Also discussed in the literature review is that the activation of octane to 1-octanol is found to be highly selective, leading to the assumption that no by-products were generated (Olaofe et al., 2013). This implies that the

most important output for this first reaction step is the amount of alcohol produced which can undergo further valorisation. Because the temperature is set at 20°C, the conversion of the alkane can only be impacted by the reactor residence time and so the impact of this needed to be investigated, as seen in Figure 11a below.

The results of this investigation presented by Figure 11a suggest, as would be expected, that increasing the residence time of the reactor results in a higher conversion of the substrate and therefore a higher 1-octanol concentration exits the system. However, an infinitely large residence time would be inefficient and economically infeasible as the greater volume required would outweigh the slight improvement in conversion achieved. Therefore, a decision was made to limit the residence time of the alkane activation reactor to 200 h as this value still enables suitable alcohol production, as demonstrated by the concentration profile presented in Figure 11b. This reactor configuration using the chosen residence time and temperature will provide enough 1-octanol to the second reaction step for alcohol oxidation to take place, while any unreacted octane passing through the system can be recycled after being separated from the products in further downstream processing.

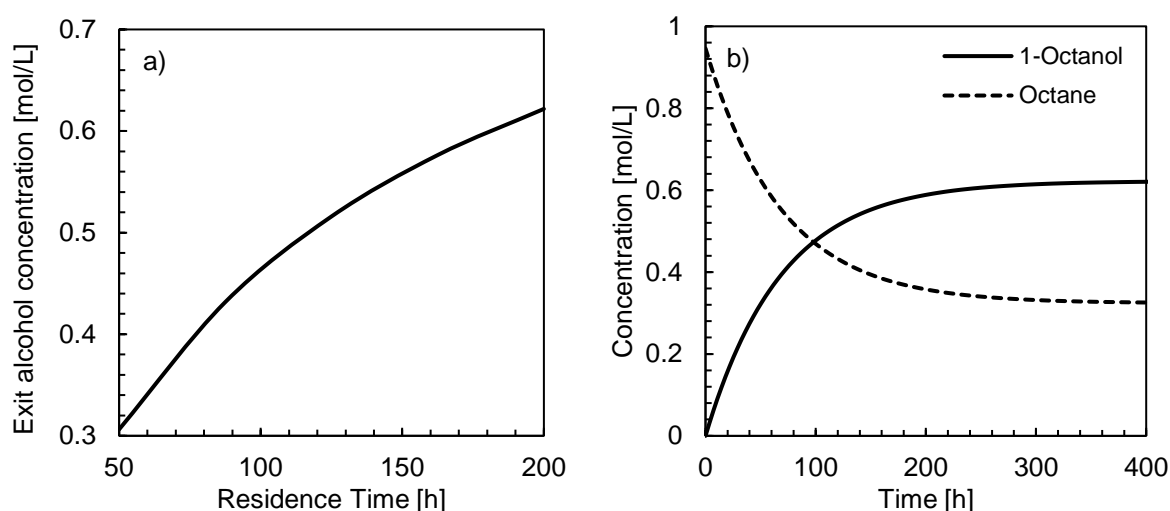


Figure 11: **a)** Exit alcohol concentration as a function of residence time. **b)** Concentration profiles for 1-octanol and octane in the alkane activation reactor.

After successfully creating a model for the first step of a two-pot process, it is now possible to use the stream produced by this reaction to begin to simulate the performance of the second step. However, an important factor to consider when attempting to link the two separate reaction steps is that their respective rates of alcohol formation and consumption need to be closely matched. This is required to ensure that the overall process operates continuously, fully employing the bio and chemical catalysts present in each of the respective reactors. If the rates are of significantly different magnitudes, there will be underutilised catalysts in one of the pots, leading to a less efficient system. Therefore, because the rate of the first reaction has already been set through the choice of residence time and temperature, the second reactor must be designed to match this rate.

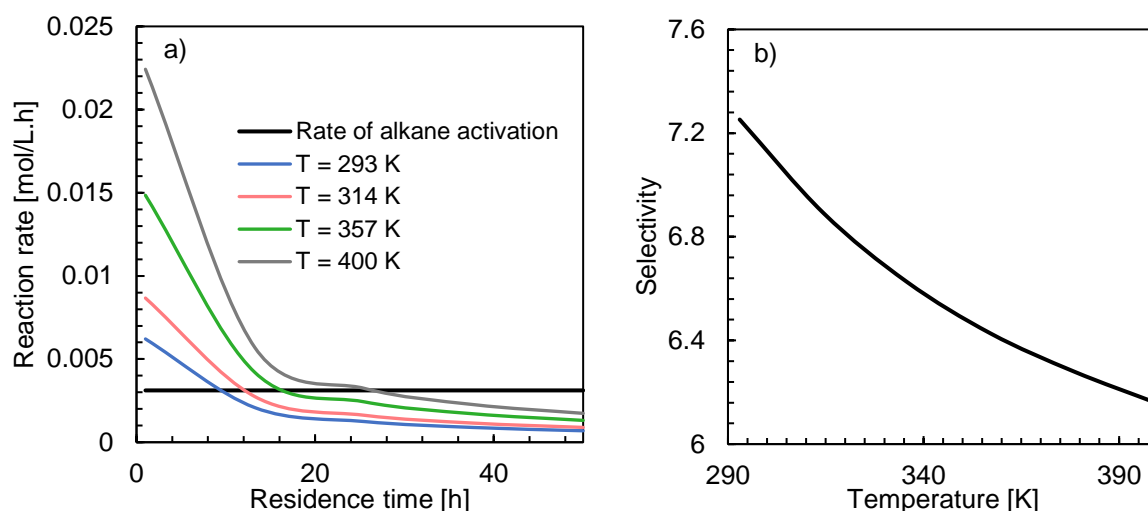


Figure 12: **a)** Matching rate of alcohol formation to alcohol consumption at different temperatures as a function of residence time. **b)** Selectivity to the aldehyde as a function of temperature.

The operation of the Au/Pd catalyst used in alcohol oxidation is less sensitive to changes in temperature than the CYP153A6 enzyme and so it is possible to vary the temperature of the second reaction to ensure that the rate of alcohol consumed is equal to the rate of alcohol formed. The effect temperature has on the kinetics of the alcohol oxidation is discussed within the reaction mechanism section of model development. The rate of consumption of alcohol within the second reaction is also dependent on the reactor's residence time, thus this can also be adjusted to ensure that there is a suitable matching of rates between the pots. The impact of both reaction temperature and residence time on the rate of alcohol consumption can be seen in Figure 12a above where various combinations of the two have been compared to the rate of the alcohol formed through bioactivation. This rate of alcohol formation was taken as the steady-state value for the biotransformation as this is the rate achieved while the process is operating in a continuous manner, as is the case during commercial production.

The analysis presented in Figure 12a demonstrates that the rate of alkane activation can be matched to the rate of alcohol consumption in the second pot at certain residence times and associated temperatures. The higher the residence time of the second reactor, the higher the temperature required to match the rate of the biocatalysed alkane hydroxylation. Therefore, a decision needs to be made around which of these combinations of temperature and residence time is preferred for the oxidation of 1-octanol to octanal. Due to the fact that the generation of aldehydes is a fine chemical synthesis, it is important to ensure that a relatively selective product is obtained. It must be noted that the selectivity reported in subsequent results is defined as the ratio of the desired octanal product to the undesired octanoic acid by-product.

The over oxidation of the formed aldehydes to produce carboxylic acid by-products is what could potentially reduce the selectivity of the system. Therefore, the impact of temperature on the selectivity of the octanal produced relative to octanoic acid generated is seen in Figure 12b. The highest selectivity to aldehyde is achieved at the lowest possible temperature of 20°C, indicating that this is the preferred condition at which to operate the alcohol oxidation reaction. Based on this temperature and Figure 12a, the optimal residence time for the second

reactor in the two-pot system is 10.2 h and it will therefore operate at 20°C with this residence time. The final decision concerning the operation of the alcohol oxidation step is the aeration rate of oxygen fed to the system to be used as the oxidising agent. The oxygen gas (O_2) reacts with the alcohol in a one-to-one ratio and thus the oxygen needs to be fed in at least this ratio to the system to ensure it is not limiting the reaction. However, the specific feed concentration of oxygen for the system needs to be chosen while keeping in mind the selectivity of aldehyde produced. The impact of varying aeration rate on the selectivity achieved can be found in Figure 13a and from this relationship, an optimal O_2 concentration can be determined.

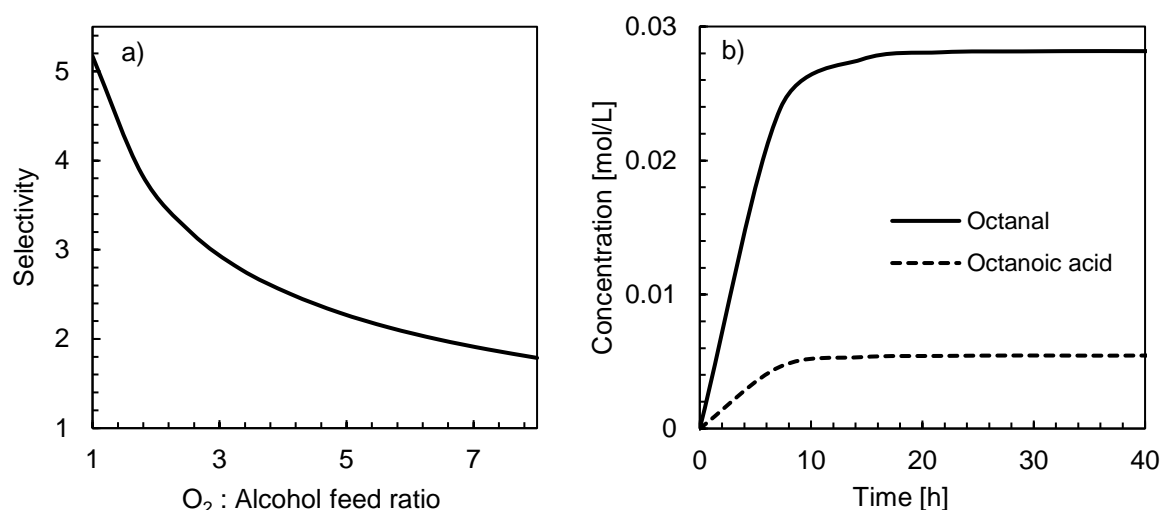


Figure 13: **a)** Selectivity to the aldehyde as a function of the aeration rate. **b)** Concentration profiles for octanal and octanoic acid in the alcohol oxidation reactor.

The results of the investigation into varying aeration rate shown in Figure 13a clearly demonstrates that a 1:1 ratio of oxygen compared to the alcohol entering the second pot results in the highest selectivity to octanal and thus this is the feed ratio which will be used for the final reactor model. This conclusion is in line with the mechanism of alcohol oxidation proposed in the model development section of the report where the secondary oxidation occurs as a result of excess oxygen being present, favouring the formation of the carboxylic acid rather than the desired aldehyde product.

Once the feed concentrations, residence time and temperature of the second step in the two-pot process have been specified, it is possible to evaluate the ultimate performance of the system. Figure 13b shows this in the form of concentration profiles for both octanal and octanoic acid where the high selectivity to the desired aldehyde product can be observed. Essentially, the two-pot system is able to generate a selective product and reduce the costs of downstream processing required. The overall yield can be improved by recycling any unreacted alkanes or alcohols to ensure that a sufficient target production rate can be met.

4.4. One-pot system

After having completed the design of a two-pot reactor system, the next stage is to investigate the potential of combining the two distinct reaction steps into a one-pot configuration to

improve the efficiency of the process and reduce the required capital costs. One of the challenges with implementing a one-pot system is to find a feasible window of operating conditions that favours the performance of both reactions. However, the analysis into the two-pot process has shown that an optimal output is achieved when both reactions take place at 20°C, increasing the possibility of a one-pot system operating at this temperature being effective for the activation and valorisation of alkanes to aldehydes. A representation of the how a one-pot system would be set up is displayed in Figure 14 below.

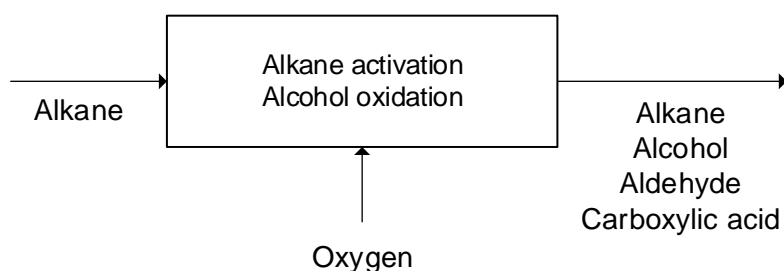


Figure 14: Simple representation of one-pot process.

As the temperature of the one-pot system has already been determined, the other major reaction variables which can be manipulated are the oxygen aeration rate and the reactor residence time. As with the two-pot system, the most important output to maximise is the selectivity of the aldehyde product as this is what is favoured for fine chemical synthesis. Therefore, the impact of both oxygen concentration and residence time of the reactor on this selectivity needs to be determined and this relationship is what is represented in Figure 15a.

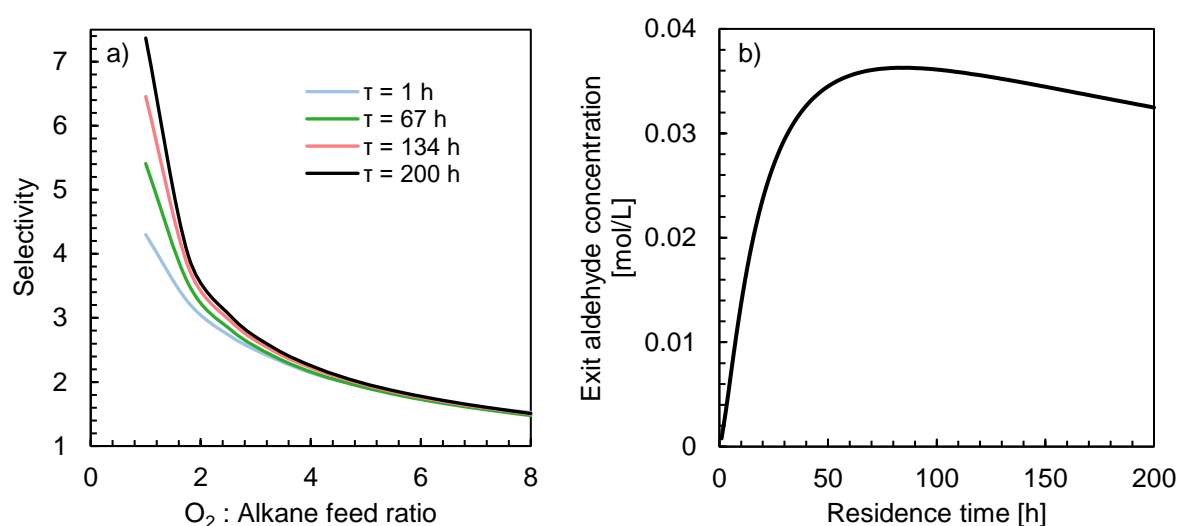


Figure 15: **a)** Selectivity to the aldehyde at different residence times as a function of aeration rate in a one-pot system. **b)** Exit aldehyde concentration as a function of residence time in the one-pot system.

There is a significant impact on the aldehyde selectivity with a changing initial O_2 concentration as demonstrated by Figure 15a. As the aeration rate increased, the ratio between octanal and octanoic acid decreased, resulting in a less selective overall process. As discussed in the analysis of the two-pot configuration, this result is explained by the proposed mechanism where the aldehyde formed from the alcohol can undergo a secondary oxidation to a carboxylic acid if there is sufficient O_2 present to act as the oxidising agent for this reaction. Figure 15a also shows that at a low aeration rate, the selectivity is improved by increasing the residence time of the reactor.

However, as indicated by Figure 15b, a maximum production rate of octanal is achieved at a specific residence time of 83 h. Therefore, if the residence time is taken at this point and an equimolar O_2 : alkane ratio is maintained then a selective aldehyde product can be generated with the maximum possible yield. The ultimate result of the one-pot reactor model can be seen in the concentration profiles presented below in Figure 16.

The final concentration profiles presented in Figures 16a and 16b demonstrate that a significant amount of the octane fed to the system is activated using the biocatalyst to form 1-octanol. This 1-octanol is then valorised to the more profitable octanal product at a high selectivity. The implication of having a selective system is that the costs of any downstream processing required are reduced and a relatively pure product can be generated.

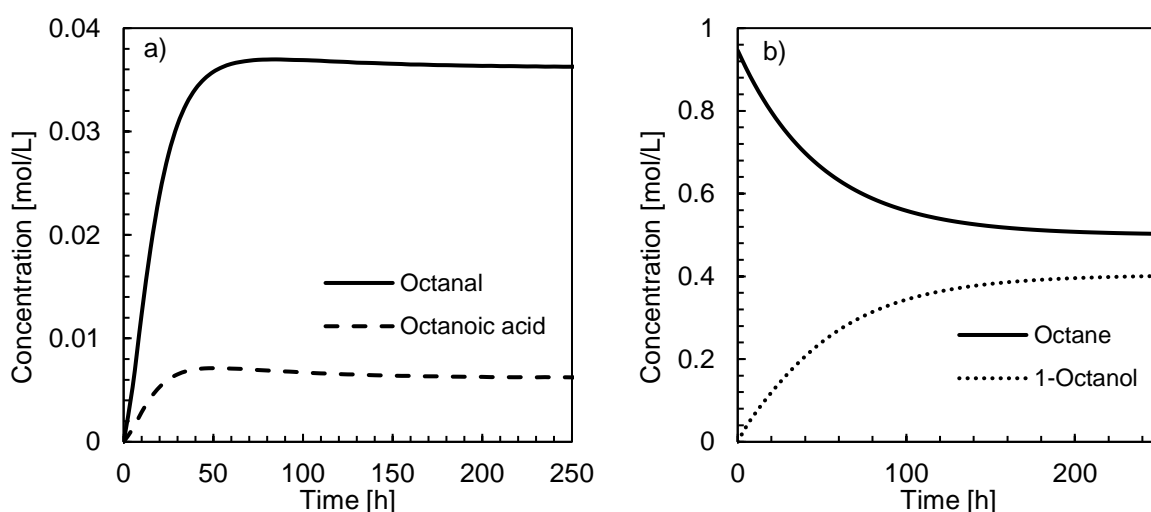


Figure 16: Concentration profiles in the one-pot system for **a)** octanal and octanoic acid and **b)** octane and 1-octanol.

There is still a significant amount of unreacted octane and 1-octanol as shown above and therefore the overall conversion of the system can be improved through the use of recycle streams. The preliminary results presented within this section show that the one-pot system appears to be feasible. However, the outputs of the model must be compared to those achieved using a two-pot configuration to effectively determine whether the one-pot route is feasible for the conversion of low value alkanes to aldehydes.

4.5. Model limitations

When analysing the results achieved by both the one-pot and two-pot processes, it is important to be aware of what assumptions were made and how this may limit the effectiveness of the modelling work done. As was discussed in the literature review, it has been found that the organic substrate and product within the bioactivation reaction (octane and 1-octanol respectively) can lead to enzyme inhibition due to toxicity effects (White et al., 2017). However, this potential lack of activity of the enzyme due to the high initial excess concentration of alkane was not fully investigated for the purposes of this study. Potential deactivation of the chemical catalyst used for the alcohol oxidation was also not taken into account. There was also no modelling done to predict the interaction between the enzyme and the chemical catalyst in the two-pot system and any decreases in process efficiency that may arise as a consequence. The negative interaction would likely be minimal with the use of a bio-supported catalyst for the valorisation of the alcohol, but for the synthetically supported catalyst, as was used in the one-pot and two-pot models, this might become more of a concern. All of these potential scenarios which have not yet been explored would likely lead to a decrease in both the yield and selectivity of the aldehyde product and thus these possibilities must be understood in more detail when drawing any final conclusions from the results presented by this study.

Another potential limitation within the work completed is the assumption that both one-pot and two-pot systems would follow ideal mixing. This assumption was made to simplify the reactor models and allow preliminary conclusions to be drawn. As with the potential enzyme and catalyst inhibition, the impacts of imperfect mixing should be investigated in greater detail in the future to better understand the true nature of the one-pot process and whether it is a feasible route for the activation of alkanes to aldehydes. The final assumption which was used for both scenarios is that the temperature of all reactor systems remained constant throughout. This assumption was made due to the low conversions achieved in both reactions and the minimal generation of energy as a result. The reactions occurring within both the one-pot and two-pot processes are also conducted in an aqueous solution, minimising the impacts of heat generation on temperature change due to the ability of water to act as a heat sink as a result of its high specific heat. Because the activation of alkanes in particular is highly sensitive to changes in the reaction environment due to the use of biological enzymes as catalysts, any slight temperature fluctuations can have significant impacts on the performance of this reaction. Therefore, the validity of the isothermal assumption should be confirmed by conducting a full energy balance for the system during the next phase of the investigation into the feasibility of a one-pot process.

4.6. Comparison of modelling results

Despite the limitations of the models discussed in the previous section, there are some important results presented which can guide the decision into whether a one-pot process is a feasible route for the creation of a valuable aldehyde product from an alkane feedstock. The comparison between the two configurations needs to be done based on the yield and selectivity of octanal produced as this will provide an understanding into the revenue which can be generated and the relative costs of downstream processing. Using an initial excess octane feed for the one-pot system, it was determined that a 0.036 M outlet concentration of octanal could be achieved with a selectivity of 6.0 relative to the amount of octanoic acid

produced. This can be compared to what is produced by the two-pot process using the same initial octane concentration. In this configuration, 0.028 M of octanal is in the effluent stream while the selectivity of the aldehyde to the carboxylic acid is now 5.2.

These results suggest that the one-pot approach is more feasible than the two-pot for the activation and valorisation of alkanes. The higher yield of product based on the initial feed achieved in one-pot indicates that a larger revenue can be generated when attempting to sell the higher value aldehyde commercially. The improved selectivity also favours the choice to use a one-pot process as the stream leaving the reactor system will have a lower concentration of octanoic acid, resulting in lower downstream processing costs needed to obtain a high purity octanal product.

The use of one reactor to complete the full conversion from octane to octanoic acid naturally results in a reduced capital investment than the two reactors required for the two-pot process. The total reactor volume in the one-pot system will also be lower as the total residence time for this configuration is 83 h, while 210 h in total residence time is required for the two pots. Using a volumetric feed flowrate basis of 1 000 L/h, a simple comparison between capital costs and potential revenues between the two scenarios can be completed and a summary of these results can be seen in Table 8 below. The use of the one-pot process could potentially reduce the initial capital expenditure by 52% while also increasing the revenue generated by 29%, assuming that all the aldehyde produced can be recovered (Alfa Aesar, 2020). The sample calculations explaining how these values were determined can be found in Appendix C (Seider et al., 2009). However, the key conclusion to be drawn is that for the given process, a one-pot approach is more desirable than the traditional two-pot system.

Table 8: Summary of capital costs and potential revenues for each reactor system.

| Reactor | | Capital Cost [R] | Potential revenue [R/annum] |
|----------------|---------------------------|------------------|-----------------------------|
| One Pot System | | 14 840 000 | 229 000 000 |
| Two Pot System | Alkane activation reactor | 26 810 000 | 178 100 000 |
| | Alcohol oxidation reactor | 4 148 000 | |

It must also be noted that both approaches operate at the same temperature of 20°C and thus there is no significant difference between them in the operating costs needed to achieve these operating conditions. As mentioned previously however, it does suggest a feasible region to operate the one-pot process that favours both the alkane activation and alcohol oxidation. This further strengthens the case that a one-pot solution is preferred to solve the problem posed at the outset of this study.

5. CONCLUSIONS

The goal of this study was to investigate the reaction kinetics of a bio-chemo tandem process utilising an inert alkane feedstock and determine if it would be feasible to conduct the two reactions in a one-pot system. It was determined through a review of the relevant literature to use a combination of alkane activation using CYP153A6 and alcohol oxidation with a catalyst comprising of Au and Pd nanoparticles. This route is advantageous because it makes use of the high selectivity and mild process conditions in the biotransformation step as well as the flexibility provided by the chemical catalyst for the subsequent valorisation of the initial product. The potential mechanisms for each of these steps and the reaction kinetics were investigated in great detail to determine if it would be possible to operate them together in a one-pot process under the same conditions.

The hypotheses selected prior to the model development stage of the study were based on the information available in literature and were selected to guide decisions taken in the project work to produce valid conclusions. The first hypothesis was that the alkane activation step would be limited by the mass transfer of the organic substrate from the organic phase to the aqueous phase where the enzyme is located and therefore where the reaction takes place. This was confirmed in the development of the reaction mechanism, where the mass transfer limitation was found to be more accurate than either the Michaelis-Menten or interfacial adsorption models. Therefore, based on the initial results presented by this study this hypothesis appears to be true and thus it is possible to take corrective action in the implementation of the process to ensure that the effect of mass transfer limitations can be minimised. As discussed in the literature review section this can be done by increasing reactor agitation or decreasing enzyme concentration, but the increased agitation must be done keeping in mind that the microorganism is sensitive to high shear forces and may be permeabilised as a result.

The second hypothesis was the one-pot process would be more feasible than the two-pot, which was also confirmed by the results presented within the study. A feasible operating region of 20°C for the one-pot system was determined which favoured both the production and consumption of alcohol to selectively produce aldehydes from alkanes. This one-pot process achieved a greater yield of aldehyde with a better selectivity than the two-pot equivalent, allowing for larger revenues to be generated and reducing the downstream processing costs required to obtain a higher purity product. The use of a one-pot configuration also reduces the capital costs associated with installing reaction vessels, making the use of a one-pot process even more favourable and leading to the conclusion that the hypothesis is true based on the information which has been presented in this report.

Although the use of a one-pot system seems to be more favourable, it is recommended that a more thorough techno-economic analysis be undertaken to more accurately understand the impacts of any downstream processing costs. This will also provide a clearer picture of whether the revenue generated from the aldehyde production is sufficient to justify the costs associated with installing and operating the reactor and downstream processing units. This techno-economic evaluation can also investigate the benefits of implementing a recycle of unreacted feed material to achieve a higher overall conversion of alkane substrate and improve the yield of the aldehyde. A greater understanding of the feasibility of using a one-pot system will be gained, and any other technical issues, such as inhibition and catalyst

interaction, which may reduce the effectiveness of the process can be better appreciated. This can guide any decisions on whether or not it is worth implementing the one-pot activation and valorisation of alkanes on a larger scale.

A final recommendation to be made is that certain results, such as the octanal production rate and selectivity, be reported for a transient system and not only at steady state conditions. This will provide greater knowledge of the specifics of the process and what impacts there are on its effectiveness if there are slight variations in its operation. Ultimately though, this report has considered many different aspects of the tandem bioactivation of alkanes and chemical oxidation of alcohols and it can be concluded that the combination of these two processes into a one-pot system is potentially feasible and should be further investigated.

6. REFERENCES

Alfa Aesar. 2020. *A10901 Octanal 98%*.

Bennett, J.A., Mikheenko, I.P., Deplanche, K., Shannon, I.J., Wood, J. & Macaskie, L.E. 2013. Nanoparticles of palladium supported on bacterial biomass: New re-usable heterogeneous catalyst with comparable activity to homogeneous colloidal Pd in the Heck reaction. *Applied Catalysis B: Environmental*. 140–141:700–707. DOI: 10.1016/j.apcatb.2013.04.022.

Bhagavan, N.V. & Ha, C.-E. 2011. Enzymes and Enzyme Regulation. In *Essentials of Medical Biochemistry*. DOI: 10.1016/b978-0-12-095461-2.00006-0.

CChange. 2020. *Distribution of products for the alkane activation using a chemical catalyst*.

Centre for Bioprocess Engineering Research. 2020. *Alkane activation data*.

Creamer, N.J., Mikheenko, I.P., Yong, P., Deplanche, K., Sanyahumbi, D., Wood, J., Pollmann, K., Merroun, M., et al. 2007. Novel supported Pd hydrogenation bionanocatalyst for hybrid homogeneous/heterogeneous catalysis. *Catalysis Today*. 128(1-2 SPEC. ISS.):80–87. DOI: 10.1016/j.cattod.2007.04.014.

Davis, R.J., Davis, S.E., Ide, M.S. & Davis, R.J. 2013. Selective oxidation of alcohols and aldehydes over supported metal nanoparticles. 15(1). DOI: 10.1039/c2gc36441g.

Deplanche, K., Mikheenko, I.P., Bennett, J.A., Merroun, M., Mounzer, H., Wood, J. & Macaskie, L.E. 2011. Selective Oxidation of Benzyl-Alcohol over Biomass-Supported Au / Pd Bioinorganic Catalysts. 1110–1114. DOI: 10.1007/s11244-011-9691-0.

Dimitratos, N., Villa, A., Wang, D., Porta, F., Su, D. & Prati, L. 2006. Pd and Pt catalysts modified by alloying with Au in the selective oxidation of alcohols. 244:113–121. DOI: 10.1016/j.jcat.2006.08.019.

Fogg, D.E. & Santos, E.N. 2004. Tandem catalysis: a taxonomy and illustrative review. 248:2365–2379. DOI: 10.1016/j.ccr.2004.05.012.

Funhoff, E.G., Bauer, U., Witholt, B. & Beilen, J.B. Van. 2006. CYP153A6 , a Soluble P450 Oxygenase Catalyzing Terminal-Alkane Hydroxylation. 188(14):5220–5227. DOI: 10.1128/JB.00286-06.

Galvanin, F., Sankar, M., Cattaneo, S., Bethell, D., Dua, V., Hutchings, G.J. & Gavriilidis, A. 2018. On the development of kinetic models for solvent-free benzyl alcohol oxidation over a gold-palladium catalyst. *Chemical Engineering Journal*. 342(August 2017):196–210. DOI: 10.1016/j.cej.2017.11.165.

Grabner, B., Schweiger, A.K., Gavric, K., Kourist, R. & Gruber-Woelfler, H. 2020. A chemo-enzymatic tandem reaction in a mixture of deep eutectic solvent and water in continuous flow. *Reaction Chemistry and Engineering*. 5(2):263–269. DOI: 10.1039/c9re00467j.

Gröger, H. & Hummel, W. 2014. Combining the “two worlds” of chemocatalysis and biocatalysis towards multi-step one-pot processes in aqueous media. *Current Opinion in Chemical Biology*. 19(1):171–179. DOI: 10.1016/j.cbpa.2014.03.002.

Hartman, R.L. 2020. Flow chemistry remains an opportunity for chemists and chemical engineers. *Current Opinion in Chemical Engineering*. 29:42–50. DOI: 10.1016/j.coche.2020.05.002.

Huang, H., Denard, C.A., Alamillo, R., Crisci, A.J., Miao, Y., Dumesic, J.A., Scott, S.L. & Zhao, H. 2014. Tandem catalytic conversion of glucose to 5-hydroxymethylfurfural with an immobilized enzyme and a solid acid. *ACS Catalysis*. 4(7):2165–2168. DOI: 10.1021/cs500591f.

Jenkins, S. 2020. *2020 CEPCI Updates: March (Prelim.) and February (Final)*. Available: <https://www.chemengonline.com/2020-cepci-updates-march-prelim-and-february-final/> [2020, October 27].

Kanse Nitin, G., Dhanke, P.. & Thombare, A. 2012. Modeling and Simulation Study of the CSTR for Complex Reaction by Using Polymath. *Research Journal of Chemical Sciences*. 2(4):79–85.

Lohr, T.L. & Marks, T.J. 2015. Orthogonal tandem catalysis. 7. DOI: 10.1038/NCHEM.2262.

Lundemo, M.T. & Woodley, J.M. 2015. Guidelines for development and implementation of biocatalytic P450 processes. *Applied Microbiology and Biotechnology*. DOI: 10.1007/s00253-015-6403-x.

Olaofe, O.A., Fenner, C.J., Gudiminch, R.K., Smit, M.S. & Harrison, S.T.L. 2013. The influence of microbial physiology on biocatalyst activity and efficiency in the terminal hydroxylation of n-octane using *Escherichia coli* expressing the alkane hydroxylase, CYP153A6. *Microbial Cell Factories*. DOI: 10.1186/1475-2859-12-8.

Seider, W.D., Seader, J.D., Lewin, D.R. & Widagdo, S. 2009. *Product and Process Design Principles: Synthesis, Analysis and Evaluation*. Third ed.

Soussan, L., Pen, N., Belleville, M., Marcano, J.S. & Paolucci-jeanjean, D. 2016. Alkane biohydroxylation : Interests , constraints and future developments. *Journal of Biotechnology*. 222:117–142. DOI: 10.1016/j.jbiotec.2016.02.007.

Straathof, A.J.J. 2003. Enzymatic catalysis via liquid-liquid interfaces. *Biotechnology and Bioengineering*. DOI: 10.1002/bit.10688.

Villa, A., Janjic, N., Spontoni, P., Wang, D., Su, D.S. & Prati, L. 2009. Au-Pd/AC as catalysts for alcohol oxidation: Effect of reaction parameters on catalytic activity and selectivity. *Applied Catalysis A: General*. 364(1–2):221–228. DOI: 10.1016/j.apcata.2009.05.059.

White, B.E., Fenner, C.J., Smit, M.S. & Harrison, S.T.L. 2017. Effect of cell permeability and dehydrogenase expression on octane activation by CYP153A6-based whole cell *Escherichia coli* catalysts. *Microbial Cell Factories*. DOI: 10.1186/s12934-017-0763-0.

Willeman, W.F., Gerrits, P.J., Hanefeld, U., Brussee, J., Straathof, A.J.J., Van Gen, A. Der & Heijnen, J.J. 2001. Development of a process model to describe the synthesis of (R)-mandelonitrile by *Prunus amygdalus* hydroxynitrile lyase in an aqueous-organic biphasic reactor. *Biotechnology and Bioengineering*. DOI: 10.1002/bit.10002.

APPENDIX A: DETAILED EXPERIMENTAL METHODS**Alkane hydroxylation***Table A1: Raw experimental data for octane hydroxylation.*

| Growth and expression procedure | Biotransformation time (h) | Dry cell weight (gDCW/L) | Concentration of active P450 (nmol/mL) | Octanol (mM) |
|---------------------------------|----------------------------|--------------------------|--|--------------|
| 2a | 0.00 | 21.28 | 24.38 | 0.00 |
| | 3.55 | 21.84 | 7.36 | 1.41 |
| | 8.97 | 24.26 | 5.76 | 3.74 |
| | 14.43 | 22.05 | 6.03 | 8.37 |
| | 25.85 | 22.16 | 3.93 | 17.59 |
| | 48.48 | 21.37 | 4.97 | 19.44 |
| | 68.90 | 21.53 | 5.83 | 19.93 |
| 2b | 0.00 | 18.44 | 38.48 | 0.00 |
| | 3.55 | 22.11 | 17.72 | 1.48 |
| | 8.97 | 24.95 | 11.29 | 2.73 |
| | 14.43 | 21.79 | 10.32 | 13.22 |
| | 25.85 | 23.21 | 8.76 | 15.46 |
| | 48.48 | 23.42 | 10.50 | 18.31 |
| | 68.90 | 22.89 | 8.69 | 20.18 |
| 2c | 0.00 | 20.17 | 30.97 | 0.00 |
| | 3.55 | 23.95 | 22.03 | 1.16 |
| | 8.97 | 26.37 | 15.21 | 2.41 |
| | 14.43 | 25.37 | 22.20 | 12.09 |
| | 25.85 | 23.84 | 13.97 | 19.27 |
| | 48.48 | 24.68 | 17.59 | 23.13 |
| | 68.90 | 24.42 | 15.79 | 25.43 |

Table A2: Continued raw experimental data for octane hydroxylation.

| Growth and expression procedure | Biotransformation time (h) | Dry cell weight (g _{DCW} /L) | Concentration of active P450 (nmol/mL) | Octanol (mM) |
|---------------------------------|----------------------------|---------------------------------------|--|--------------|
| 2d | 0.00 | 21.22 | 25.03 | 0.00 |
| | 3.55 | 26.68 | 14.17 | 1.70 |
| | 8.97 | 25.26 | 9.25 | 8.60 |
| | 14.43 | 25.37 | 10.54 | 7.54 |
| | 25.85 | 24.79 | 9.45 | 17.33 |
| | 48.48 | 25.84 | 13.06 | 16.69 |
| | 68.90 | 24.21 | 8.82 | 28.04 |
| 2e | 0.00 | 21.28 | 21.66 | 0.00 |
| | 3.55 | 26.11 | 42.11 | 2.58 |
| | 8.97 | 26.16 | 59.69 | 1.56 |
| | 14.43 | 25.68 | 80.51 | 5.73 |
| | 25.85 | 24.63 | 36.69 | 21.09 |
| | 48.48 | 24.11 | 37.47 | |
| | 68.90 | 25.21 | 30.06 | 17.99 |
| 2f | 0.00 | 21.72 | 6.77 | 0.00 |
| | 3.55 | 27.47 | 60.31 | 1.11 |
| | 8.97 | 25.74 | 79.23 | 1.73 |
| | 14.43 | 26.47 | 82.87 | 10.82 |
| | 25.85 | 24.32 | 62.97 | 20.94 |
| | 48.48 | 26.42 | 62.63 | 30.19 |
| | 68.90 | 26.53 | 50.09 | 21.82 |

Table A3: Growth and expression procedures.

| Code | Antibiotics and Precursors |
|------|--|
| 2a | 30 mg/L kanamycin |
| 2b | 30 mg/L kanamycin 0.25 mM δ -ALA |
| 2c | 30 mg/L kanamycin 0.1 mM δ -ALA 25 μ M FeCl ₃ |
| 2d | 30 mg/L kanamycin 50 μ M FeCl ₃ |
| 2e | 30 mg/L kanamycin 0.25 mM δ -ALA 50 μ M FeCl ₃ |
| 2f | 30 mg/L kanamycin 0.5 mM δ -ALA 100 μ M FeCl ₃ |

Following on from Table A3 above, the growth and expression procedure also consisted of other steps. A 201 mL culture volume was used with 799 mL of headspace in the vial and a 2 mL inoculum. The incubation temperature was maintained at 20°C throughout the 50.2 h period of growth and expression while the agitation of the vial was completed at 150 rpm. The composition of the medium used can be seen in Table A4 below.

Table A4: Medium composition.

| Substance | Concentration |
|---|---------------|
| Tryptone | 10 g/L |
| Yeast extract | 5 g/L |
| (NH ₄) ₂ SO ₄ | 25 mM |
| KH ₂ PO ₄ | 50 mM |
| Na ₂ HPO ₄ | 50 mM |
| Glycerol | 5 g/L |
| Glucose | 0.5 g/L |
| Lactose | 2 g/L |
| MgSO ₄ | 2 mM |

Table A5: Description of bacterial strain used for octane hydroxylation.

| Host | Plasmid 1 | | Plasmid 2 | |
|-----------------|-----------|----------------|-----------|------------|
| | Name | Protein(s) | Name | Protein(s) |
| E. coli BL21DE3 | pET28b+ | A6 + FdR + Fdx | - | - |

Table A6: Description of terms used in Table A5.

| Code | Description |
|------|---|
| A6 | CYP153A6 from Mycobacterium sp HXN-1500 |
| FdR | Ferredoxin reductase from Mycobacterium sp HXN-1500 |
| Fdx | Ferredoxin from Mycobacterium sp HXN-1500 |

Table A7: Description of cell preparation procedure.

| Centrifugation conditions | Resuspension buffer | Intended cell concentration | Permeabilisation treatment |
|---------------------------|---|-----------------------------|----------------------------|
| 5 min 5000 rpm 4 °C | 25 g/L K ₂ HPO ₄ 7.7 g/L KH ₂ PO ₄ 18.4 g/L glycerol Biotransformation carried out in presence of 100 µL BEHP. | 20 g _{wcW} /L | None |

Table A8: Description of inoculum preparation procedure.

| Liquid Volume (mL) | Medium Composition | Antibiotics and Precursors | Incubation Temperature (°C) | Agitation (rpm) | Incubation Period (h) |
|--------------------|--|----------------------------|-----------------------------|-----------------|-----------------------|
| 10 | 10 g/L tryptone 5 g/L yeast extract 5 g/L NaCl | 30 mg/L kanamycin | 36 | 200 | 13.6 |

Alcohol oxidation

The experimental data for the conversion of 1-octanol to octanal over a synthetically supported Au₈₀/Pd₂₀ catalyst was sourced from Villa et al. (2009) with the experimental method being as follows. The bimetallic synthetically supported Au/Pd catalyst was prepared using a sol-gel method in order to immobilise both metal particles on the support in a specific ratio. The metal content of the catalyst was then confirmed using an inductively coupled plasma optical emissions spectroscopy (ICP) analysis and the microstructures were studied using transmission electron spectroscopy (TEM). The catalytic conversion of 1-octanol to octanal was performed in a 30 mL glass reactor at 60°C. The reactor was connected to an oxygen reservoir at 1.5 atm with the initial concentration of 1-octanol fed to the reactor was 0.3 M. The catalytic tests were done with and without sodium hydroxide (NaOH) present in the reaction vessel. However, only the tests completed without NaOH present were considered as a result of the scope of this project. The results from Villa et al. (2009) were presented as a conversion profile, as shown in Figure A1. Using the initial concentration of 0.3 M, the conversion profile was converted to the concentration-time data provided in Table A9.

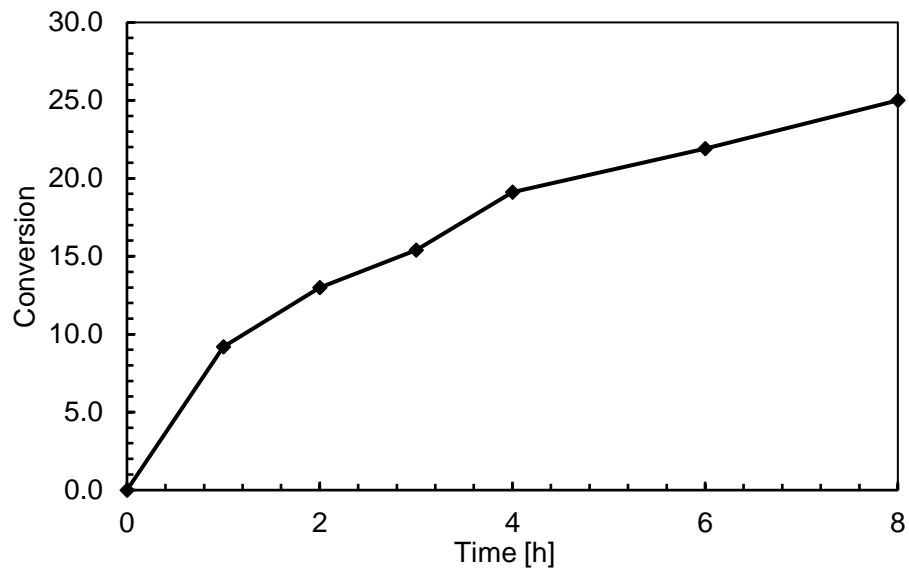


Figure A1: Conversion of 1-octanol raw data (Villa et al., 2009)

Table A9: Concentration-time data for the oxidation of 1-octanol

| Time [h] | Conversion [%] | C _A [M] |
|----------|----------------|--------------------|
| 0 | 0.00 | 0.300 |
| 1 | 9.20 | 0.2724 |
| 2 | 13.0 | 0.2610 |
| 3 | 15.4 | 0.2538 |
| 4 | 19.1 | 0.2427 |
| 6 | 21.9 | 0.2343 |
| 8 | 25.0 | 0.2250 |

APPENDIX B: ALCOHOL OXIDATION PARAMETER ESTIMATION RESULTS**Parameter estimation for Model 0***Table B1: Parameters for Model 0 as a result of non-linear regression*

| | | | |
|------------------------------|--------|----------------|--------|
| $A_0 [h^{-1}(mol/l)^{1/4}]$ | 5.8501 | $Ea_0 [J/mol]$ | 1117.6 |
| $A_1 [h^{-1}(mol/l)^{1/4}]$ | 14.067 | $Ea_1 [J/mol]$ | 1346.6 |
| $A_2 [h^{-1}(mol/l)^{-1}]$ | 4.6684 | $Ea_2 [J/mol]$ | 3851.7 |
| $A_3 [h^{-1}(mol/l)^{-2}]$ | 12.756 | $Ea_3 [J/mol]$ | 5668.7 |
| $A_4 [h^{-1}(mol/l)^{-1/4}]$ | 16.420 | $Ea_4 [J/mol]$ | 2177.2 |
| $A_5 [h^{-1}(mol/l)^{-3/4}]$ | 14.040 | $Ea_5 [J/mol]$ | 7457.5 |
| $A_6 [h^{-1}]$ | 12.596 | $Ea_6 [J/mol]$ | 4430.1 |
| $A_7 [h^{-1}(mol/l)^{-1/2}]$ | 6.4005 | $Ea_7 [J/mol]$ | 8565.2 |

Parameter estimation for Model 1*Table B2: Parameters for Model 1 as a result of non-linear regression*

| | | | |
|-----------------------------|--------|----------------|--------|
| $A_0 [h^{-1}(mol/l)^{1/4}]$ | 2.0611 | $Ea_0 [J/mol]$ | 12458 |
| $A_1 [h^{-1}(mol/l)^{1/4}]$ | 0.3666 | $Ea_1 [J/mol]$ | 1800.9 |
| $A_2 [h^{-1}(mol/l)^{1/4}]$ | 20.057 | $Ea_2 [J/mol]$ | 4242.6 |
| $A_3 [h^{-1}(mol/l)^{-1}]$ | 29.438 | $Ea_3 [J/mol]$ | 1849.0 |

APPENDIX C: CAPITAL COSTING SAMPLE CALCULATIONS

The heuristic based method used to determine the capital costs of the reaction vessels in the one and two-pot processes are outlined below (Seider et al., 2009). The CEPCI values for 2006 and 2019, which are used to account for increase in capital costs over time, are 499.6 and 619.2 respectively (Jenkins, 2020). The rand to dollar conversion used is R16.72 per dollar (Jenkins, 2020).

The calculations used to determine the capital cost of each reactor are as follows (Seider et al., 2009). Sample calculations for the one system are shown below. A basis of for the feed volumetric flowrate entering the system was taken as 1000 L/h. Assuming an operating time of 8000 h/annum, the amount of aldehyde produced annually is 36 tons/annum. This is in line with the typical fine chemical production rates outlined by Seider et al. (2009).

Table C1: Summary of information required to size each reactor

| | | | |
|-----------------------|------|--|-------|
| Volumetric Flow [L/h] | 1000 | $\rho_{\text{carbon steel}}$ [lb/inch ³] | 0.284 |
| Residence time [h] | 83 | Design pressure [bar] | 2.71 |
| Pressure [psi] | 14.7 | L/D | 2 |

The first step in sizing the reactor is to use the aspect ratio to determine the length and diameter of the reactor, assuming the reactor is cylindrical in shape. These are then used to determine the reactor wall thickness and weight (Seider et al., 2009) using the equations shown below.

$$t_{\text{wall}} = 0.022 P(\text{bar})D(\text{m}) \quad (49)$$

$$W = \pi(D + t_{\text{wall}})(L + 0.8D)t_{\text{wall}}\rho_{\text{cs}} \quad (50)$$

The following equations are then used to determine the bare module cost of the reactor. The reactor is assumed to be constructed out of carbon steel since the reactor contents are non-corrosive and carbon steel is cheaply available. Hence, the material factor (F_m) is taken as 1.

$$C_v = \exp \{7.0132 + 0.18255 \ln(W) + 0.02297 [\ln(W)]^2\} \quad (51)$$

$$C_{pl} = 361.8 \left(\frac{D}{12}\right)^{0.73960} \left(\frac{L}{12}\right)^{0.70684} \quad (52)$$


$$C_{BM} = F_{BM}(C_v F_m + C_{pl}) \left(\frac{CEPCI(2019)}{CEPCI(2006)}\right) (RD) \quad (53)$$

Where C_{BM} is the total bare module cost, F_{BM} is the bare module factor and is taken as 4.16 and RD is the rand to dollar conversion used (Seider et al., 2009).

APPENDIX D: DATA MANAGEMENT DECLARATION**CHE4045Z 2020****Project Data Management Declaration**

In the interest of transparency and ethics in research it is herewith confirmed that

1. All data generated within the project has been stored in suitable form (electronic form, but also paper copies or specimens, where appropriate) such that it remains accessible to project supervisors and examiners beyond the end of the project. Electronic data should ideally be stored in a shared cloud folder (such as Vula, Dropbox or Google Drive), as advised and administered by the project supervisor.
2. The electronic project data referred to in 1. above has been appropriately labelled and organised, and a table of contents of the relevant stored data (including a web address of the folder where this information is publicly accessible) has been prepared and included in an Appendix to the Final Report submitted by the students.
3. All data and materials handed to the students at the beginning of the project which are subject to confidentiality have been returned or, where appropriate, deleted from any of the students' personal storage devices, by instructions from the supervisor.
4. All proprietary software and/or software licences made available to the students for use in the project has been removed from any of the students' personal storage devices, by instructions from the supervisor.

| | |
|--|---|
| Project Number: 33 | Date: 10/12/2020 |
| Student 1 – Name & Student Number: Nikhil Mistry MSTNIK002 | Signature  |
| Student 2 – Name & Student Number: Joe Payne PYNERI001 | Signature  |
| Supervisor: Name: Dr Thanos Kotsiopoulos | Signature  |

APPENDIX E: ETHICS CLEARANCE

Application for Approval of Ethics in Research (EIR) Projects
Faculty of Engineering and the Built Environment, University of Cape Town

APPLICATION FORM

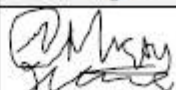
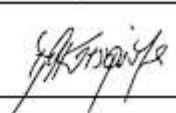
Please Note:

Any person planning to undertake research in the Faculty of Engineering and the Built Environment (EBE) at the University of Cape Town is required to complete this form **before** collecting or analysing data. The objective of submitting this application *prior* to embarking on research is to ensure that the highest ethical standards in research, conducted under the auspices of the EBE Faculty, are met. Please ensure that you have read, and understood the **EBE Ethics in Research Handbook** (available from the UCT EBE, Research Ethics website) prior to completing this application form: <http://www.ebe.uct.ac.za/ebe/research/ethics1>

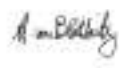
| APPLICANT'S DETAILS | | |
|--|--|------------------------|
| Name of principal researcher, student or external applicant | Nikhil Mistry Joe Payne | |
| Department | Chemical Engineering | |
| Preferred email address of applicant: | MSTNIK002@myuct.ac.za PYNERI001@myuct.ac.za | |
| If Student | Your Degree: e.g., MSc, PhD, etc. | BScEng |
| | Credit Value of Research: e.g., 60/120/180/360 etc. | 36 |
| | Name of Supervisor (if supervised): | Dr Thanos Kotsiopoulos |
| If this is a research contract, indicate the source of funding/sponsorship | Click here to enter text. | |
| Project Title | Investigating the system kinetics and thermodynamics in bio-chemo tandem systems | |

I hereby undertake to carry out my research in such a way that:

- there is no apparent legal objection to the nature or the method of research; and
- the research will not compromise staff or students or the other responsibilities of the University;
- the stated objective will be achieved, and the findings will have a high degree of validity;
- limitations and alternative interpretations will be considered;
- the findings could be subject to peer review and publicly available; and
- I will comply with the conventions of copyright and avoid any practice that would constitute plagiarism.

| APPLICATION BY | Full name | Signature | Date |
|---|----------------------------|--|--|
| Principal Researcher/ Student/External applicant | Nikhil Mistry Joe Payne |  | 02 Sep 2020 |
| SUPPORTED BY | Full name | Signature | Date |
| Supervisor (where applicable) | Dr Thanos Kotsiopoulos |  | 03 Sep 2020 Click here to enter a date. |
| APPROVED BY | Full name | Signature | Date |

Application for Approval of Ethics in Research (EIR) Projects
Faculty of Engineering and the Built Environment, University of Cape Town

| | | | |
|---|---|--|---|
| HOD (or delegated nominee) Final authority for all applicants who have answered NO to all questions in Section 1; and for all Undergraduate research (Including Honours). | Prof H von Blottnitz |  | 13/09/2020 <small>enter a date.</small> |
| Chair: Faculty EIR Committee For applicants other than undergraduate students who have answered YES to any of the questions in Section 1. | Click here to enter text. | | Click here to enter a date. |